NASA Technical Memorandum 87678

Effects of Partial Interlaminar Bonding on Impact Resistance and Loaded-Hole Behavior of Graphite/Epoxy Quasi-Isotropic Laminates

Walter Illg

JULY 1986

NASA

NASA Technical Memorandum 87678

Effects of Partial Interlaminar Bonding on Impact Resistance and Loaded-Hole Behavior of Graphite/Epoxy Quasi-Isotropic Laminates

Walter Illg
Langley Research Center
Hampton, Virginia

National Aeronautics
and Space Administration

Scientific and Technical Information Branch

1986

Symbols

Values are given in SI Units but, where considered expedient, also in U.S. Customary Units. Measurements and calculations were made in U.S. Customary Units.

d	diameter, mm
P	load, kN
P_F	load at failure, kN
$P_{\max}$	maximum load, kN
P_1	load at first damage, kN
S_b	bearing stress, MPa
S_g	remote stress, MPa
S_r	residual strength of damaged specimen, MPa
S_{ult}	ultimate strength, MPa
t	thickness, mm
V	velocity
δ	elongation of loaded hole, mm
δ_F	elongation of loaded hole at failure, mm
$\delta_{\max}$	maximum elongation of loaded hole, mm
δ_1	elongation of loaded hole at first damage, mm
ϵ	axial strain
μ_{xy}	Poisson's ratio

Abbreviations:

DCDT	direct-current differential transformer
DNF	did not fail
NDE	nondestructive evaluation

Summary

An interlaminar weakening concept that was developed to improve fracture toughness of composites was evaluated for its effects on resistance to impact and for behavior around a loaded hole. Mylar[1] sheets with 25- and 15-percent perforations were interleaved between 24 composite prepreg layers. Specimens were impacted by 13-mm-diameter aluminum spheres while under tensile or compressive loads. Failure thresholds and residual strengths were obtained. The loaded-hole specimens were tested in three configurations: bearing critical, shear critical, and tension critical. Ultrasonics and X-radiography were used to detect damage.

The tensile and compressive strengths of undamaged specimens were reduced by 36 and 30 percent, respectively, by partial bonding. Partial bonding reduced by 50 percent the velocity of impact that could be survived while under compression. Also under compression, the prestrain threshold level for failure was about one-half that under tension for all bonding percentages. Little benefit of partial bonding was uncovered for tension, and serious degradation occurred for compression.

Partial bonding reduced the maximum load-carrying capacity of all three types of loaded-hole specimens. It was concluded that, overall, the partial interlaminar bonding concept was detrimental both to impact resistance and to the bearing capacity of holes. Notwithstanding these negative results, much was learned about the effects of weakened interlaminar interfaces.

Introduction

Graphite/epoxy laminates are widely used in secondary structures such as flaps and ailerons on commercial aircraft because this material is light, strong, stiff, and commands a weight advantage over aluminum in such structures. Secondary structures are generally designed for properties other than strength, thus making strength-degradation problems of less importance. Aircraft with composite tails are in service; these too are critical in stiffness rather than strength. But in primary structures like wings and fuselages, strength is of utmost concern. There, the effects of structural damage on residual strength must be calculable to assess flight safety and repair procedures.

Residual strengths of laminates containing crack-like defects (through slits) have been studied extensively. Those data indicate that graphite/epoxy laminates are significantly weakened by slits and fail in a brittle manner with little stable crack growth. In 1964, Cook and Gordon (ref. 1) proposed that certain debonding phenomena occur ahead of cracks in tension-loaded unidirectional composites, thus abating the locally elevated fiber stresses. In 1973, Marston (ref. 2) suggested that intermittent weak bonds between fiber and matrix could enhance fracture toughness by encouraging a Cook-Gordon mechanism to create beneficial interfacial disbonding ahead of a tension crack. To evaluate this suggestion, Atkins (ref. 3) performed experiments on compact tension specimens that were fabricated using boron fibers that were intermittently coated with varnish and set in an epoxy matrix. He found up to a four-fold increase in fracture toughness.

The application of this principle to graphite/epoxy required a new concept for weakening because fibers as fine as graphite cannot be individually coated. An alternate concept was proposed by Wolf Elber (U.S. Patent No. 4,229,473) that provided weakened interlaminar planes rather than weak fiber/matrix interfaces. In his concept, thin (7 μm) perforated Mylar sheets were interleaved with graphite/epoxy prepreg; strong bonding occurs only at the perforations. Thus, total bond strength is controlled by net perforation area and hole spacing. Elber performed exploratory tests of this concept of partial interlaminar separation and reported the results in reference 4. His specimens were 150 mm wide, and the perforated Mylar was inserted in the region of the slit to within 12.5 mm of each edge. Using 40- to 50-percent bonding, he found a 60-percent increase in fracture load for centrally slitted specimens. Specimens under tensile load survived impacts for prestresses up to 375 MPa if they contained perforated Mylar. Without Mylar, specimens failed at prestresses as low as 250 MPa.

In 1977, Felbeck (ref. 5) used 1.1-, 2.2-, and 6.8-mm-diameter holes in Mylar to develop partial bonding from 0 to 100 percent in six increments. Specimens were of the double-cantilever type. Fracture toughness was increased by 190 percent for about 14-percent bonding, whereas the tensile strength was reduced by only 26 percent. In 1979, Jea (ref. 6) reported results on a larger number of modified compact tension specimens; he used only 1.1-mm-diameter holes in the Mylar. Jea found up to a four-fold increase in fracture toughness for bonding fractions of 18 and 36 percent. Surprisingly, he observed no significant difference between tensile strengths at these two bonding fractions and no loss of tensile strength due to the presence of the Mylar interleaves themselves. Jea suggested that optimum bonding for T300/5208 graphite/epoxy quasi-

[1] Mylar: Registered trademark of E. I. du Pont de Nemours & Co., Inc.

isotropic laminates occurred at about 18-percent perforations.

Finally, in 1980, Felbeck and Jea (ref. 7) performed additional tests on modified compact tension specimens and concluded that fracture toughness was increased from about 100 to about 500 kJ/m^2, whereas tensile strength dropped from 500 to 400 MPa. Reference 8 supports the concept of interlaminar weakening to improve fracture toughness. In that paper, Poe concluded that easy crack-tip damage raised the fracture toughness of graphite/epoxy, whereas strong, tough matrices inhibited such damage and depressed the fracture toughness.

These studies showed that the intermittent bonding concept can significantly enhance fracture toughness yet maintain a reasonable tensile strength. Before this concept is considered for composite structures, its effects on other desirable properties must be determined. In the present work, the capability to carry load while being subjected to impact was examined experimentally for T300/5208 laminates. In addition, the effects of partial bonding on the behavior of specimens with load-bearing holes were investigated.

Materials and Specimens

Quasi-isotropic laminates were laid up with 24 plies of T300/5208 prepreg and were cured using the manufacturer's standard autoclave procedure. Nine panels that were 172 cm by 30 cm were fabricated and ultrasonically scanned. Specimens were laid out as shown in figure 1 and were cut into the shapes shown in figure 2. The impact specimens were labeled with two digits; the first is the panel number and the second is the number of the specimen within the panel. For example, "3-1" denotes the first specimen in panel 3. Partial interlaminar bonding was attained by alternating prepreg plies with perforated Mylar sheets. The hole patterns in the Mylar sheets are shown in figure 3. Holes for both patterns had the same diameter. Therefore, varying hole spacing produced two different bonding fractions. The presence of the 7-μm-thick Mylar sheets added approximately 8 μm to the thickness of each ply. The extra 1 μm was probably due to excess epoxy retained in the laminate. Thus, the normal 24-ply laminate thickness averaged 3.12 mm, whereas those with Mylar sheets averaged 3.32 mm. The perforation fractions that were estimated using a $\times 30$ microscope were 25 and 15 percent. Throughout this paper, the three degrees of bonding are referred to as "100-percent bonded", "25-percent bonded", and "15-percent bonded".

The pin-loading holes in these loaded-hole specimens were machined with an ultrasonic drill. Radiographs showed that machining damage around the holes was insignificant. Three types of loaded-hole specimens were tested (fig. 2): bearing critical (B), shear critical (S), and tension critical (T). The loaded-hole specimens were labeled with a letter and a number. The letter refers to the critical mode of failure and the number is the panel number. Thus, S-2 is the shear-critical specimen from panel number 2.

Apparatus

Impact Tests

The impact apparatus shown in figures 4 and 5 is the same system that was used for the impact work published in reference 9. A 1.3-cm-diameter aluminum sphere was propelled within a steel barrel by air pressure. The desired velocity was controlled by presetting the pressure-control valve. Figure 6 shows how air pressure is related to velocity for various hole sizes in the orifice plate. At the exit end of the barrel, a two-diode detector senses the passage of the sphere. An event timer indicates the elapsed time between the two diodes from which exit velocity may be accurately calculated. The impact event is initiated by opening the quick-acting solenoid air valve.

Shown in figure 5(b) are the steel antibuckling frames. They are 2.5 cm thick and 15 cm square overall with a 7.6-cm-square window centrally located. Calculations showed that an undamaged 24-ply laminate would not buckle within a 7.6-cm window under axial compressive preloads up to the highest preload contemplated for the present test series. Figure 5(c) shows the gun aligner used to aim the gun at the center of each specimen. The transparent safety shield helped retain the aluminum spheres after impact. A new sphere was used for each impact. The centering clamps held the antibuckling frames in line with the grips. Figure 5(d) shows the reverse side of the test setup. A DCDT (direct-current differential transformer) was mounted to the upper grip to monitor the distance between grips.

Axial tensile or compressive loads produced by a hydraulic cylinder beneath the lower grip were sensed by a load cell that controlled the loads through servovalves. The plastic-lined box grips relied on friction to transfer loads to the specimens. Six 0.5-in-diameter screws in each grip were torqued to 100 ft-lbf. The two halves of the antibuckling frame were held against the specimen with light pressure by carefully torquing eight screws connecting the two frames.

Loaded-Hole Tests

Because the primary purpose of the tests of loaded-hole specimens was to track damage accumulation, each test was interrupted periodically for NDE. Hence, the loads measured after the first loading cycle were probably influenced by previous load cycles.

A special apparatus for continuously measuring elongation of loaded holes is shown in figure 7. A drop of glue held the wire to the edge of the hole. This method was conceived by Crews and is described fully in reference 10. One end of the specimen was gripped by friction. Load was introduced into the hole by a clevis with a 0.25-in-diameter steel bolt that was torqued to 50 in-lbf, a moderate torque for this size of bolt. Hole-bolt clearance was 0.005 in. Two steel washers separated the clevis from the specimen. The washers and the bolt were slotted so that a bent wire could bear on the edge of the hole and transmit the displacement to two transducers attached to the clevis. Thus, as a tensile load was applied, the transducers measured the changing diameter of the hole in the direction of loading. The clevis and bolt were too stiff to perturb this measurement materially.

Loading was by a hydraulically actuated testing machine using hole-elongation control to avoid sudden destruction of the specimens. In some cases, this strategy did not prevent sudden fracture. Loading rate was slaved to produce a hole-elongation rate of 0.005 mm/s. To monitor the accumulation of damage, each specimen was periodically unloaded, injected with X-ray opaque dye (zinc iodide), and radiographed. Specimens were radiographed whenever significant damage was indicated by a sudden noise and/or a sudden drop in load. This procedure was continued until either gross failure occurred or deflection increased while the load remained constant—essentially a pseudoplastic condition.

Results and Discussion

Tensile Tests of Undamaged Specimens

Tensile tests were performed on 4.8-cm-wide specimens to determine the basic properties of this layup. Strains were sensed with a foil x-y gauge at the center of the back and front faces. The results are given in table I. Typical tensile stress-strain curves are sketched in figure 8. It is apparent that the surface plies (45°) of the laminates containing Mylar sheets delaminated early and voided the gauges. The sudden decrease in strains at the breaks indicates that 45° surface plies had decoupled from the others. The 100-percent-bonded laminates maintained integrity until final fracture. The breaks in the stress-strain curves for 25- and 15-percent-bonded specimens occurred at strains that were proportional to their bonding fractions, thus showing that they were triggered by the weakened interfaces. It should be noted that throughout this paper a "standard ply" thickness of 0.140 mm was assumed, which leads to a 24-ply standard thickness of 3.36 mm. A standard thickness is desirable because the strength and stiffness of a laminate with a plastic matrix is overwhelmingly dependent on the fiber content regardless of the proportion of plastic to fiber. Thus, when stresses are calculated herein, the effective area is the standard thickness multiplied by the actual laminate width.

Figure 9 shows photographs of a typical tensile failure for each bonding percentage. For 100-percent bonding, the fracture damage was confined to a short distance from the transverse separation. In contrast, the partially bonded specimens delaminated to considerable lengths, almost reaching the grips in the 15-percent-bonded case. These failures illustrate that weakened interlaminar bonds encourage widespread delamination.

Compressive Tests of Undamaged Specimens

Tests for compressive properties were done on specimens of the same width as those used for impact tests (9.9 cm). The results are given in table II. The first number in the specimen designation is the panel from whence it came. The specimens for compressive property tests were made from different panels than those for the impact specimens. However, auxiliary tensile tests showed that these three panels (15, 16, and 17) were nearly identical to the impact panels (1 to 9) and so may be considered equivalent for general comparisons of data. Compressive strengths dropped monotonically with the percent of bonding.

Impact and Residual-Strength Tests

Since prestrain could not be monitored on the specimens because of interference with the impactor, the prestrains were set up for each test assuming that the distance between grips changed in correspondence with the total deflection of the specimen. After the impact tests were completed, this assumption was checked with an undamaged specimen that was instrumented across the midline with three foil gauges on each face. The specimen was loaded to 89 kN tension (or 269 MPa stress) and compression using the same carefully controlled gripping procedure that was used for the impact tests. The results are shown in figure 10. It was found that the average of six foil gauges produced a linear load-strain trace in both tension and compression. But the DCDT between

grips produced decidedly nonlinear curves. It is probable that the specimens and the plastic grip pads deformed significantly within the grips during loading; the higher the load, the greater the proportion of deformation within the grips. Consequently, the actual prestrains were obtained after the fact using the actual loads and the moduli from tables I and II and Hooke's law. Thus, specimens were impacted under tensile or compressive prestrains varying from 0.0018 to 0.0065.

Impact velocities were varied from 12 to 75 m/s. The object was to define a boundary that separates those specimens that survived from those that collapsed or fractured during impact. Table III summarizes the impact test results; figure 11 shows the results for impact under tensile prestrain. No differences were discerned for the survival threshold in tension for the 100-percent-, 25-percent-, or 15-percent-bonded specimens. Some improvement had been expected in light of the gains in fracture toughness brought about by partial bonding as reported in references 4 to 7. Also, Kennedy (ref. 11), using 16-ply quasi-isotropic laminates, showed increases in fracture strength up to 37 percent for specimens of widths from 2.2 to 10.1 cm with slits of one-third the width.

Apparently, increased fracture toughness does not necessarily translate into improved impact resistance. More troubling is the improvement in impact resistance found by Elber (ref. 4) for two specimens that contained Mylar interleaves with 40-percent perforations made with a computer-card puncher. The greater percent of bonding may have contributed to that improvement, but another factor may be that his Mylar interleaves extended only to 12.5 mm from the edges. This feature may have prevented premature failure of the 45° plies at the edges.

In contrast to the tensile results, figure 12 for compressive prestrains shows a serious degradation of impact resistance for the partially bonded specimens. The specimens with 25-percent and 15-percent bonding were equally degraded. The thresholds for compressive prestrain, even for 100-percent bonding, were much lower than those for tensile prestrain for the same impact velocities. These results for compression are not unexpected because it is known that the compressive strength of composites is quite sensitive to delaminations. The data suggest that failures will not occur below a certain prestrain level regardless of velocity. This agrees with previous research which suggested that as penetration velocity is approached, the damage done by impacts levels off and actually decreases somewhat (ref. 12).

In tension the limit is about 0.0047. This is about one-half the ultimate strain for undamaged specimens. The prestrain level for the limit in compression (fig. 12) of 0.0024 is close to the 0.0028 reported in reference 13 for the same material but twice as thick (48 plies). The thicker material was more resistant to impact collapse as evidenced by the knee of the threshold curve being at a velocity of 110 m/s, whereas in the present tests it was at 50 m/s. The threshold for failure when impacted under load provides guidelines for in-flight survivability. Having survived a damaging impact, it is of interest to ascertain the capabilities of the weakened but intact specimens. The remainder of the discussion will concern the damage detected by ultrasonic C-scan inspection and the residual strengths of the survivors. The survivors of the impact tests were scanned ultrasonically to detect the extent of impact damage. The C-scans are shown in figure 13. The outline of the window in the antibuckling guide is shown as dashed lines. The attenuation ratio between the light and dark areas was 6 dB. The X-radiographs are arranged in order of increasing area of delamination. The most noticeable features of the scans for tension prestrain are the "ears" that protrude at 45°. No ears occurred for compressive prestrains. Similar impact ears were reported in the literature. For example, reference 14 reported C-scans with ears for 8-ply graphite/epoxy that was impacted with a 12.7-mm sphere while clamped in a 101-mm circular ring. Although those specimens were not preloaded, membrane deformation during impact induced some tensile inplane stress. Apparently, impact in the presence of tensile stress will produce C-scan ears parallel to a 45° ply. The ears are probably elongated delaminations at one interface that projected beyond the symmetric delaminations at other interfaces.

The surviving specimens were tested for residual tensile or compressive strengths using the same antibuckling frame that was used for the impact tests. The results are listed in table III and are shown in figure 14 plotted against velocity. In the figure the prestresses during impact are indicated as short horizontal bars. The threshold curves from figures 11 and 12 are also shown with the ordinate converted from strain to stress using Young's modulus. Two specimens, labeled "(1)", were impacted in compression but were failed in tension. For tension (fig. 14(a)), two failure points lie below the threshold. The point marked "(1)" was impacted while under compression, but that does not explain its low strength because another such test (just to the left) fell well above the threshold. For compression (fig. 14(b)), failing stresses were all above the threshold curves. It appears that the residual strengths are not related to the threshold curves in a simple way.

Sense of preload	Bonding, percent	Number of correlations for -				
		Maximum possible	Damage area		Damage width	
			Velocity	Prestrain	Velocity	Prestrain
Tension	100	1	1	0	1	1
	25	2	2	0	2	0
	15	3	3	0	3	0
Total		6	6	0	6	1
Compression	100	6	4	1	4	2
	25	3	2	2	2	1
	15	2	0	1	1	0
Total		11	6	4	7	3

Residual strengths are also given in table III as fractions of the strengths of undamaged specimens. The tensile strength of undamaged 100-percent-bonded material exceeded the compressive strength by 6 percent. The effect of 25-percent and 15-percent bonding, in the absence of damage, was to lower the tensile strengths to 84 and 64 percent, respectively. (See fig. 8.) For compression, the 25- and 15-percent-bonding strengths were lowered to a single level—70 percent.

The relation between residual strengths and damage areas is shown in figure 15. Generally, strengths decreased with increased damage area for all three degrees of bonding, as indicated by the faired trend lines. In tension, the 100-percent strengths fell considerably below those for 25 and 15 percent for a given damage area. In compression, strengths for 100-percent bonding fell, with the lowest values found for partially bonded specimens. These two observations could indicate that for the same areas of delamination, fiber failure caused by impact was more extensive in the 100-percent specimens. It appears that partial bonding improves the residual strengths of the survivors somewhat. C-scanning can detect the projected areas of delamination, but it cannnot detect the extent within individual layers or detect fiber failures. It is clear that this method of NDE is not appropriate for determining residual strengths after impact.

Significance of Velocity Versus Prestrain

The extent of delamination is affected by both the velocity of impact and the prestrain levels. The relative importance of these two factors on damage could not be determined directly because of the paucity of data. However, two representations of the data giving evidence toward this end will now be discussed.

First, the senses of changes in velocity and prestrain (positive, neutral, or negative) are compared with the senses of changes in damage area and damage width, as seen by the C-scans. Delamination areas and widths are plotted, respectively, in figures 16 and 17 against velocities and prestrains. The velocity data are connected with solid lines and the prestrain data are connected with dashed lines. Correlations are indicated by positive slopes because damage is expected to increase monotonically with increases of an effective parameter. A tabular summary of correlations is shown in the table above. For tension preload, velocity had the maximum possible number of correlations with damage area and width; prestrain correlated only once with width and never with area. For compression, velocity correlated in slightly more than one-half the events, whereas prestrain correlated in about one-third. This comparison supports velocity as the major delamination driver when prestrain is tensile and as a somewhat less dominant driver when prestrain is compressive.

Second, the residual tensile and compressive strengths of the impact survivors were plotted in figure 18 against velocity and prestrain. Lines were drawn through the symbols whenever a definite trend was indicated. Velocity again correlated well, this time with residual strength, in both tension and compression. The prestrain data show a general trend that is contrary to expectations. That is, strength increased with prestrain levels. Two specimens that were impacted under compression but pulled in tension to failure (marked "C") fell outside the trends. If these two data points are discounted, impact damage at a given velocity weakened the 100-percent-bonded specimens to a greater extent in tension than the partially bonded specimens.

Therefore, the evidence from figures 16, 17, and 18 indicates a strong correlation between impact velocity and specimen damage in both tension and compression; prestrain had minimal effect and then only in compression.

Although these data showed little increase in impact resistance under tensile preload and a serious degradation for compressive preloads, they are still very useful for evaluating the general effects of weakened interfaces on some laminate properties.

Loaded-Hole Tests

Recall that to monitor the accumulation of damage, each specimen was unloaded and radiographed whenever significant damage was indicated by sight or sound. Table IV summarizes the results in terms of peak loads and deflections for both the first cycle and the final cycle and in terms of the overall maximum values obtained for each specimen. The shapes of the load-deflection curves are shown schematically in figure 19. Some of the shear-critical and tension-critical specimens failed in the first cycle without warning. However, if the first cycle did not cause failure of the bearing-critical or shear-critical specimens, repetitions expanded the hysteresis loops. None of the bearing-critical specimens failed completely but instead developed apparent pseudoplasticity; that is, further deflections did not increase the load. Conversely, all the tension-critical specimens failed without showing signs of pseudoplasticity. Four shear-critical specimens developed pseudoplasticity and five failed completely. The effect of partial bonding in the bearing case was to increase the maximum hole elongation δ_{max} prior to pseudoplasticity. For the shear-critical and tension-critical cases, not much effect of partial bonding on the cyclic loop shapes is seen. For the tension-critical and shear-critical specimens, modes of damage other than bearing were activated before reaching the bearing first-damage load P_1. Other features are better expressed in subsequent figures.

The effects of partial bonding on maximum bearing stress ($S_b = P_1/td$) can be seen in figure 20. For all three specimen types, the maximum stresses were highest for 100-percent bonding. For bearing and shear specimens, the maxima were reduced by 18 and 28 percent for 25 and 15 percent bondings, respectively. Bearing strength is dependent on interply integrity because it is essentially a compressive phenomenon. Therefore, the lower strengths for partial bonding of bearing-critical specimens are expected because of the weakened interfaces.

Also shown in figure 20 are the values of S_b from reference 15 for thinner (16-ply) quasi-isotropic loaded-hole specimens of the same material and design as the present specimens but fully bonded (points A and B in fig. 20). For bearing-critical specimens, the first-damage stress is much lower for the referenced 16-ply material although the maximum stresses are equal. Probably, the initial local bearing damage is delayed in the thicker material because of the extra lateral support. The partially bonded thicker material also carried higher bearing stresses than the thinner fully bonded material. Conversely, for shear-critical tests, the stresses for initial damage are similar although the maximum stress is higher for the thicker laminate. For tension-critical tests, both initial and maximum stresses are unaffected by thickness.

Damage was visualized with radiographs taken after each cycle using a contrast-enhancing zinc iodide solution. The radiographs of the damaged regions of all specimens are shown in figures 21, 22, and 23 together with the loads and hole elongations that were reached prior to each radiograph. The radiographs for three of the peaks for specimens B-4 and B-5 are not shown in figure 21 for convenience. The letters B, S, and T followed by a number refer to specimen type and panel number, respectively. In figure 21(a) note that all radiographs of the 100-percent-bonded bearing-critical specimens except one were made with a gold chloride enhancer. One can see by the final view of specimen B-3 that zinc iodide penetrates deeper and shows more damage.

The accumulation of damage as revealed by these radiographs proceeded differently in the three types of specimens, as described in the following discussion:

First, the bearing-critical specimens (fig. 21): for 100-percent bonding, damage apparently began as semicircumferential local crushing followed by wavelike spreading from the loaded side of the hole. Partial bonding encouraged the early appearance of 45° shear strips (which did not reach any edge) in concert with the wavelike spreading.

Second, the shear-critical specimens (fig. 22): for 100-percent bonding, early damage appeared as small tension cracks transverse to the load followed by 45° shear strips that ran to the end and edges. The partially bonded specimens generated no tension cracks but developed 45° shear strips as in the 100-percent-bonded case.

Third, the tension-critical specimens (fig. 23): for 100-percent bonding, damage again started as tiny tension cracks. However, in this case, the tension cracks were accompanied by short 45° shear cracks. The shear cracks grew as the tension cracks advanced to the edges. For the partially bonded specimens, no initial tension cracks or bearing crushing appeared before final failure. However, delaminated strips developed along the longitudinal edges of the specimens and extended to the ends of the specimens. In general, this edge damage was greater for those specimens with partial bonding. The following table summarizes the senses of the effects of partial

Parameter	Specimen critical in -		
	Bearing	Shear	Tension
Load			
First damage, P_1 . . .	−	0	+
Failure, P_F	(a)	−	−
Maximum, P_{max} . . .	−	−	−
Hole elongation			
First damage, δ_1 . . .	−	0	+
Failure, δ_F	(a)	−	−
Maximum, δ_{max} . . .	+	−	−

[a]Test terminated before complete failure.

bonding on measured loads and hole elongations (from table IV). In bearing-critical specimens, partial bonding reduced the loads and elongations for first damage but the maximum elongations were significantly increased. As noted earlier, this is not surprising because bearing resistance depends on interlaminar strength to maintain the fibers in alignment, and the greater values of δ_{max} were the result of softening due to damage spread. In shear-critical specimens, the first-damage loads and elongations were unaffected by partial bonding. This would suggest that the initial damage was primarily interfiber rather than interlaminar. Maximum loads and failure loads and elongations fell with partial bonding. The reductions in elongation showed that bearing was not a major contributor to the shear-critical failures. In tension-critical specimens, the greater loads and elongations to exhibit first damage indicate that partial bonding enhanced the load at first damage without reducing initial stiffnesses. Failure loads (maximum loads) were only slightly depressed, a result supporting the notion that phenomena other than bearing or interlaminar shear were operative in these specimens. As in other published fracture data, weakened interlaminar bonding can beneficially blunt the effects of a stress raiser when tension is the major mode of failure (ref. 8).

These data for loaded holes show that partial bonding can raise the load for first damage in cases where a joint is tension critical. On the other hand, all other load milestones were degraded or unaffected.

Conclusions

An interlaminar weakening concept that was developed to improve fracture toughness of graphite/epoxy laminates was evaluated for its effects on resistance to impact and for its behavior around a loaded hole. The following conclusions were based on this study:

Impact Tests

1. The threshold for impact fracture under tensile loads was unaffected by partial bonding. The minimum prestrain for fracture was 0.0047 at velocities greater than 50 m/s. This is about one-half the ultimate strain for undamaged specimens.

2. Under compression, the minimum prestrain for collapse was about one-half that for tension.

3. Under compression, partial bonding seriously degraded the impact resistance of the laminate. The survivable velocity of impact was lowered by a factor of 2.

4. Damage was influenced more by the velocity of impact than by the prestrain level.

5. For undamaged specimens, partial bonding lowered the tensile and compressive strengths to 64 and 70 percent, respectively, when compared with 100-percent-bonded laminates.

6. Residual tensile strengths after impact were generally higher for partially bonded specimens than for fully bonded specimens.

Loaded-Hole Tests

1. Partial bonding reduced the maximum load-carrying ability for bearing-critical specimens, shear-critical specimens, and, to a lesser extent, tension-critical specimens.

2. First-damage loads were increased by partial bonding in the tension-critical case although maximum loads were somewhat depressed.

3. Maximum hole elongations were increased for bearing-critical specimens but were decreased for shear-critical and tension-critical specimens by partial bonding.

4. When shear and tension failures were precluded, bearing damage led to pseudoplastic behavior.

NASA Langley Research Center
Hampton, VA 23665-5225
March 13, 1986

References

1. Cook, J.; and Gordon, J. E.: A Mechanism for the Control of Crack Propagation in All-Brittle Systems. *Proc. R. Soc. London*, ser. A, vol. 282, no. 1391, Dec. 8, 1964, pp. 508–520.
2. Marston, T. U.: The Effect on Controlled Intermittent Interfacial Bonding on the Tensile Properties and Fracture Toughness of a Boron-Epoxy Composite. Ph.D. Thesis, Univ. of Michigan, 1973.
3. Atkins, A. G.: Intermittent Bonding for High Toughness/High Strength Composites. *J. Mater. Sci.*, vol. 10, no. 5, May 1975, pp. 819–832.

4. Elber, Wolf: *Toughening of Graphite-Epoxy Composites by Interlaminar Perforated Mylar® Films.* NASA TM-78643, 1978.
5. Felbeck, D. K.: *Fiber Reinforced Solids Possessing Great Fracture Toughness: The Role of Interfacial Strength, Supplement 4.* NASA CR-154022, 1977.
6. Jea, Li-Chung: Fracture Toughness of Graphite/Epoxy Composite Laminates Enhanced by the Intermittent-Interlaminar-Bonding Strength. Ph.D. Diss., Univ. of Michigan, 1979.
7. Felbeck, David K.; and Jea, Li-Chung: *Increased Fracture Toughness of Graphite-Epoxy Composites Through Intermittent Interlaminar Bonding.* NASA CR-159198, 1980.
8. Poe, C. C., Jr.: *Fracture Toughness of Fibrous Composite Materials.* NASA TP-2370, 1984.
9. Rhodes, Marvin D.: *Impact Tests on Fibrous Composite Sandwich Structures.* NASA TM-78719, 1978.
10. Crews, J. H., Jr.: Bolt-Bearing Fatigue of a Graphite/Epoxy Laminate. *Joining of Composite Materials,* K. T. Kedward, ed., ASTM Spec. Tech. Publ. 749, 1980, pp. 131–144.
11. Kennedy, John M.: Fracture Behavior of Hybrid Composite Laminates. *A Collection of Technical Papers, Part 1: Structures and Materials—AIAA/ASME/ASCE/AHS 24th Structures, Structural Dynamics and Materials Conference,* May 1983, pp. 68–73. (Available as AIAA-83-0804.)
12. Husman, G. E.; Whitney, J. M.; and Halpin, J. C.: *Residual Strength Characterization of Laminated Composites Subjected to Impact Loading.* AFML-TR-73-309, U.S. Air Force, Feb. 1974. (Available from DTIC as AD A121 106.)
13. Williams, Jerry G.; Anderson, Melvin S.; Rhodes, Marvin D.; Starnes, James H., Jr.; and Stroud, W. Jefferson: *Recent Developments in the Design, Testing and Impact-Damage Tolerance of Stiffened Composite Panels.* NASA TM-80077, 1979.
14. Cantwell, W.; Curtis, P.; and Morton, J.: Post-Impact Fatigue Performance of Carbon Fibre Laminates With Non-Woven and Mixed-Woven Layers. *Composites,* vol. 14, no. 3, July 1983, pp. 301–305.
15. Crews, J. H., Jr.; and Naik, R. V. A.: *Failure Analysis of a Graphite/Epoxy Laminate Subjected to Bolt Bearing Loads.* NASA TM-86297, 1984.

TABLE I. EFFECTS OF PERFORATED MYLAR SHEETS ON TENSILE PROPERTIES

[$[45/90/0/-45/-45/0/90/45/45/90/0/-45]_s$; two tests per panel]

Bonding, percent	Panel	S_{ult}, MPa (a)	Strain	Poisson's ratio, μ_{xy}	Young's modulus, GPa (b)
100	1	[c]437	9375×10^{-6}	[c]0.296	50.5
	2	479	9308	.302	51.4
	3	489	9518	.296	51.4
Average		468	9400×10^{-6}	0.298	51.1
25	4	411	[c,d]8470×10^{-6}	0.257	50.1
	5	403	[d]8150	.295	50.5
	6	405	[d]7675	.297	50.7
Average		406	8098×10^{-6}	0.283	50.4
15	7	359	[d]5000×10^{-6}	0.294	52.9
	8	363	[d]5340	.293	52.1
	9	358	[d]5025	.278	51.5
Average		360	5122×10^{-6}	0.288	52.2

[a]Specimen standard cross section: 4.80 cm by 0.335 cm = 1.61 cm^2.
[b]Initial slope.
[c]One test only.
[d]Surface plies separated at these strains, thus voiding further measurements.

TABLE II. EFFECTS OF PERFORATED MYLAR SHEETS ON COMPRESSIVE PROPERTIES

[$[45/90/0/-45/-45/0/90/45/45/90/0/-45]_s$; tested with 7.6-cm-square window]

Bonding, percent	Specimen (a)	S_{ult}, MPa (b)	Young's modulus, GPa (c)
100	15-1	511	50.4
	15-2	481	
Average		496	
25	16-1	340	49.4
	16-2	363	
Average		352	
15	17-2	355	
	17-3	347	49.6
Average		351	

[a]No compressive-strength tests run on panels 1 to 9.
[b]Specimen standard cross section: 9.88 cm by 0.335 cm = 3.31 cm^2.
[c]Initial slope; blank spaces indicate no data obtained.

TABLE III. RESULTS OF IMPACT AND RESIDUAL-STRENGTH TESTS

(a) Tensile prestrain

Bonding, percent	Specimen (a)	Prestrain	Preload, kN	Velocity, m/s	Kinetic energy, J	Failed on impact?	Damage[b]		Residual strength, MPa (c)	Strength fraction
							Area, cm^2	Width, cm		
100							0	0	[d]484	1.00
	3-5	5701×10^{-6}	97.0	44.8	3.01	Yes				
	2-5	6407	109.0	48.8	3.57	Yes				
	3-4	4879	83.0	33.8	1.72	No	2.2	2.8	312	.64
	1-6	4924	82.3	49.4	3.66	No	13.4	6.2	290	.60
25							0	0	[d]407	1.00
	6-5	5899×10^{-6}	99.0	40.9	2.50	Yes				
	4-5	5819	96.5	48.8	3.57	Yes				
	6-4	4892	82.1	58.2	5.09	Yes				
	4-4	4764	79.0	48.2	3.48	No	29.4	6.1	399	.98
	5-4	4230	70.7	57.9	5.03	No	37.2	8.1	314	.77
	5-5	4313	72.1	65.5	6.44	No	43.4	8.4	239	.59
15							0	0	[d]360	1.00
	7-1	4826×10^{-6}	84.5	48.8	3.57	Yes				
	8-2	5607	96.7	31.4	1.48	No	11.6	3.9	410	1.14
	9-1	5778	98.5	40.2	2.43	No	(e)	(e)		
	9-2	4986	85.0	47.3	3.35	No	35.9	6.3	362	1.01
	8-1	4100	70.7	54.6	4.47	No	39.7	7.0	326	.91
	7-2	4015	70.3	75.3	8.51	No	65.4	8.9	309	.86

[a]First number is panel of origin.
[b]Damage detected by C-scanning.
[c]Based on nominal thickness of 3.35 mm and area of 2.21 cm^2.
[d]Average tensile strength of 2-in-wide specimens (from table I).
[e]Delaminated far beyond window.

TABLE III. Concluded

(b) Compressive prestrain

Bonding, percent	Specimen	Prestrain	Preload, kN	Velocity, m/s	Kinetic energy, J	Failed on impact?	Damage[a]		Residual strength, MPa	Strength fraction
							Area, cm^2	Width, cm		
100							0	0	[b]496	1.00
	1-5	-5425×10^{-6}	−90.5	33.8	1.72	Yes				
	1-4	−4466	−74.5	40.9	2.50	Yes				
	1-1	−4106	−68.5	47.0	3.31	Yes				
	2-4	−3669	61.2	47.0	3.31	Yes				
	2-1	−2745	−45.8	48.8	3.57	Yes				
	1-2	−4508	−75.2	25.9	1.01	No	.19	.5	−512	1.03
	3-1	−2679	−44.7	36.3	1.97	No	3.28	2.3	−317	.64
	2-2	−3357	−56.0	40.9	2.50	No	5.81	3.4	−200	.40
	3-2	−2398	−40.0	45.7	3.14	No	3.55	2.7	−191	.39
	2-3	−2242	−37.4	47.6	3.39	No	6.97	3.4	[c]431	1.20
	1-3	−1798	−30.0	50.6	3.84	No	12.9	5.3		
	3-3	−2320	−38.7	52.7	4.17	No	10.9	4.2	−141	.28
25							0	0	[b]351	1.00
	5-1	-3425×10^{-6}	−56.0	18.0	0.49	Yes				
	6-2	−2832	−46.3	24.7	.92	Yes				
	6-3	−2391	−39.1	28.0	1.18	Yes				
	5-2	−2856	−46.7	30.5	1.39	Yes				
	4-1	−3620	−59.2	31.1	1.45	Yes				
	5-3	−4458	−72.9	14.0	.30	No	2.77	2.3	−231	.66
	4-3	−3510	−57.4	11.9	.21	No	.58	1.3	−383	1.09
	4-2	−2813	−46.0	18.0	.49	No	4.26	2.8	−266	.76
	6-1	−1878	−30.7	18.3	.50	No	3.27	2.2	−242	.68
15							0	0	[b]351	1.00
	8-4	-4538×10^{-6}	−74.5	18.0	0.49	Yes				
	9-3	−2778	−45.6	21.0	.66	Yes				
	8-3	−2765	−45.4	25.0	.94	Yes				
	7-4	−4337	−71.2	13.7	.28	No	4.32	2.8	−425	1.21
	7-3	−3588	−58.9	15.5	.36	No	7.58	3.2	−370	1.05
	9-4	−2235	−36.7	21.3	.68	No	4.39	3.2	−150	.43

[a]Damage detected by C-scanning.

[b]Average compressive strength for 4-in-wide specimens (from table II).

[c]Tested for residual strength in tension.

TABLE IV. RESULTS OF LOADED-HOLE TESTS

Bonding, percent	Panel order	Bearing-critical specimen				Shear-critical specimen				Tension-critical specimen			
		Panels 1 to 9			Average	Panels 1 to 9			Average	Panels 1 to 9			Average
Values of P_1, kN													
100	1, 2, 3	19.9,	(a),	18.8	19.4	12.6,	12.6,	12.7	12.6	10.2,	11.4,	11.0	10.9
25	4, 5, 6	17.3,	17.7,	17.0	17.3	(b),	14.1,	13.3	13.7	12.0,	11.6,	11.4	11.7
15	7, 8, 9	15.9,	15.9,	15.1	15.6	13.6,	11.8,	12.4	12.6	11.8,	12.2,	12.2	12.1
Values of δ_1, mm													
100	1, 2, 3	0.299,	(a),	0.284	0.292	0.197,	0.198,	0.169	0.188	0.159,	0.200,	0.169	0.176
25	4, 5, 6	.255,	.260,	.250	.255	(b),	.207,	.216	.212	.185,	.190,	.189	.188
15	7, 8, 9	.273,	.280,	.245	.266	.193,	.165,	.179	.179	.190,	.206,	.198	.198
Vaues of P_F, kN													
100	1, 2, 3					17.3,	17.2,		17.2	12.8,	12.3,	12.9	12.7
25	4, 5, 6		(c)			15.0,	14.3,	(c)	14.7	12.0,	11.6,	12.4	12.0
15	7, 8, 9					13.6,	(c),		13.6,	11.7,	12.3,	12.2	12.1
Values of δ_F, mm													
100	1, 2, 3					0.408,	0.310,		0.359	0.253,	0.249,	0.257	0.253
25	4, 5, 6		(c)			.253,	.255,	(c)	.254	.185,	.190,	.228	.201
15	7, 8, 9					.193,	(c),		.193	.209,	.216,	.198	.208
Values of P_{max}, kN[d]													
100	1, 2, 3	22.1,	(a),	21.2	21.7	**17.3**,	**17.2**,	17.9	17.5	**12.8**,	**12.3**,	**12.9**	**12.7**
25	4, 5, 6	17.3,	17.7,	17.0	17.3	**15.0**,	**14.3**,	14.6	14.6	**12.0**,	**11.6**,	**12.4**	**12.0**
15	7, 8, 9	15.9,	15.9,	15.1	15.6	**13.6**,	12.4,	12.4	12.8	**11.7**,	**12.3**,	**12.2**	**12.1**
Values of δ_{max}, mm[d]													
100	1, 2, 3	0.575,	(a),	0.539	0.557	**0.408**,	0.314,	0.378	0.367	**0.253**,	**0.249**,	**0.257**	**0.253**
25	4, 5, 6	.979,	1.043,	1.057	1.026	(b),	**.255**,	.335	.295	**.185**,	**.190**,	**.228**	**.201**
15	7, 8, 9	.939,	.550,	.473	.654	**.193**,	.385,	.400	.326	**.209**,	**.216**,	**.198**	**.208**

[a]No data recorded.
[b]Data for first cycle not recorded.
[c]Tests terminated before complete failure because of pseudoplasticity.
[d]Bold maximum values coincide with failure values.

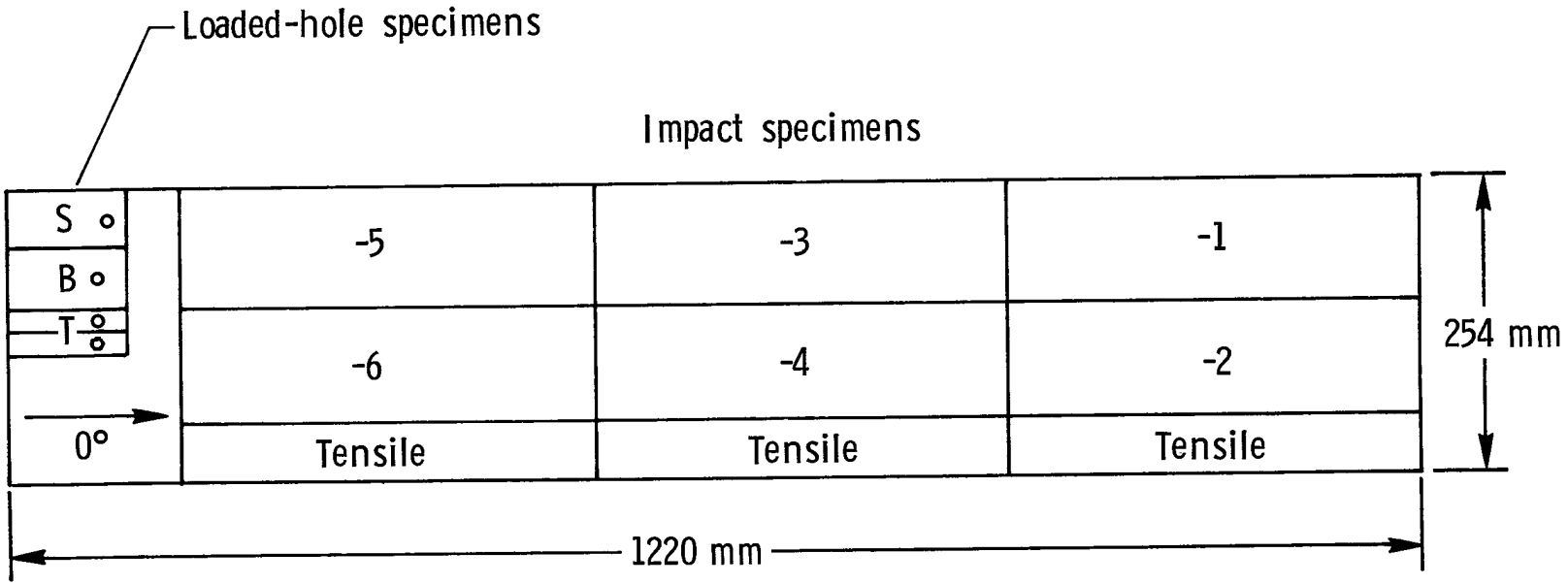

Figure 1. Composite panel layout. 24 plies.

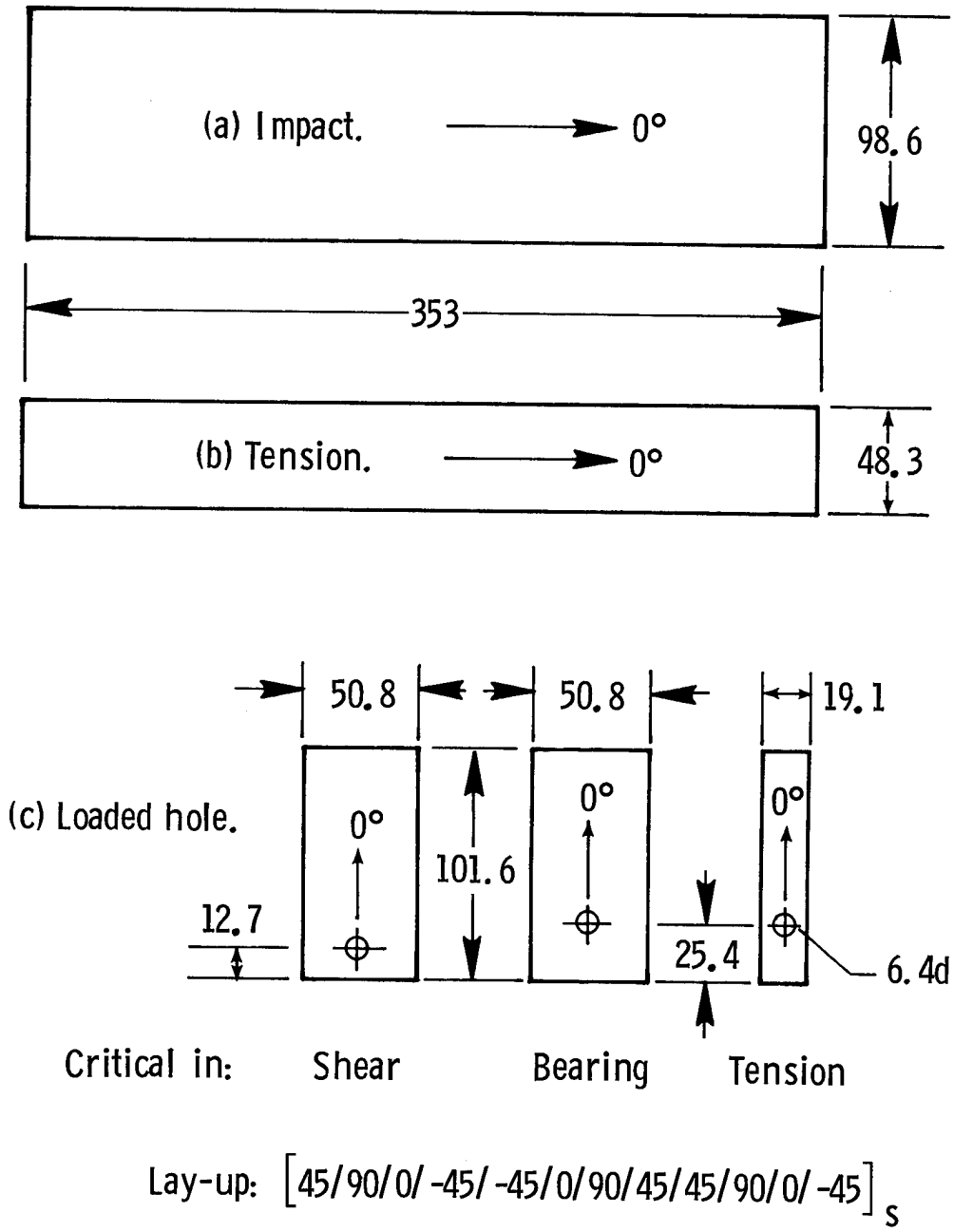

Figure 2. Specimen shapes. Dimensions are given in millimeters unless otherwise noted.

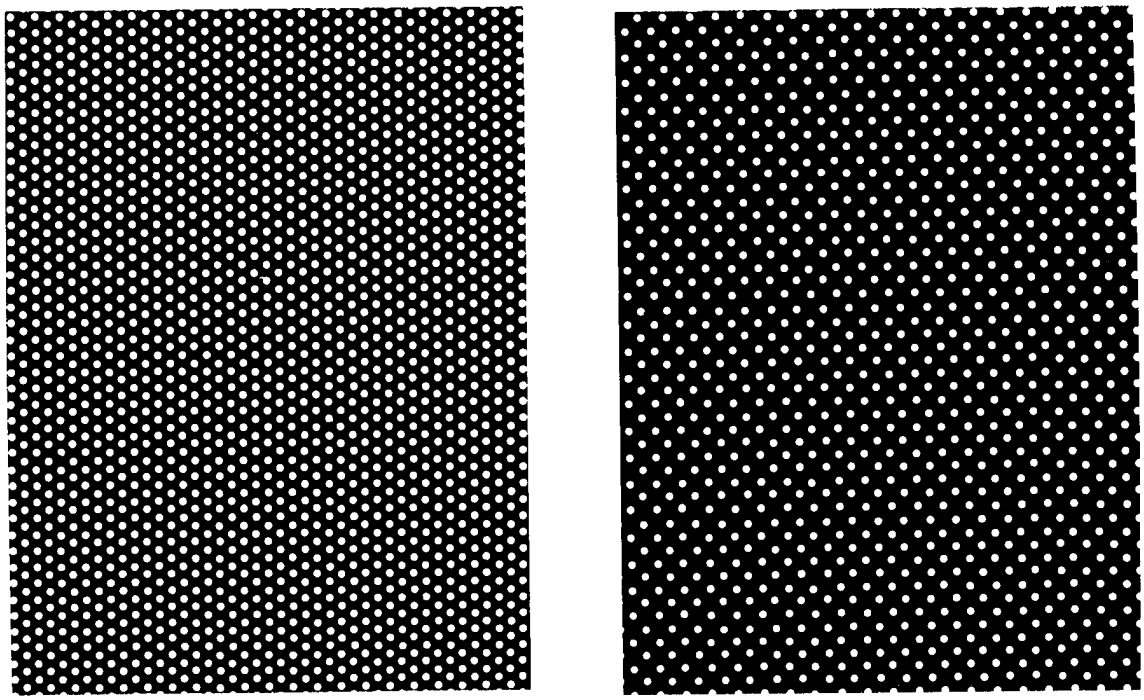

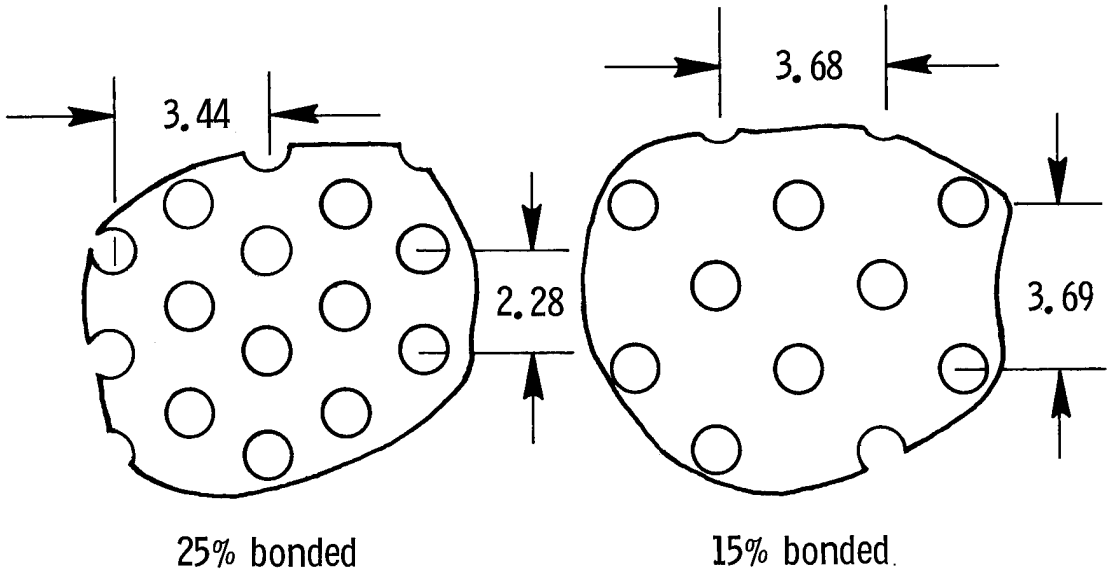

L-86-322

Figure 3. Hole patterns in 7-μm-thick Mylar sheets. Hole diameter is 1.12 mm; dimensions are given in millimeters; photographs are full scale.

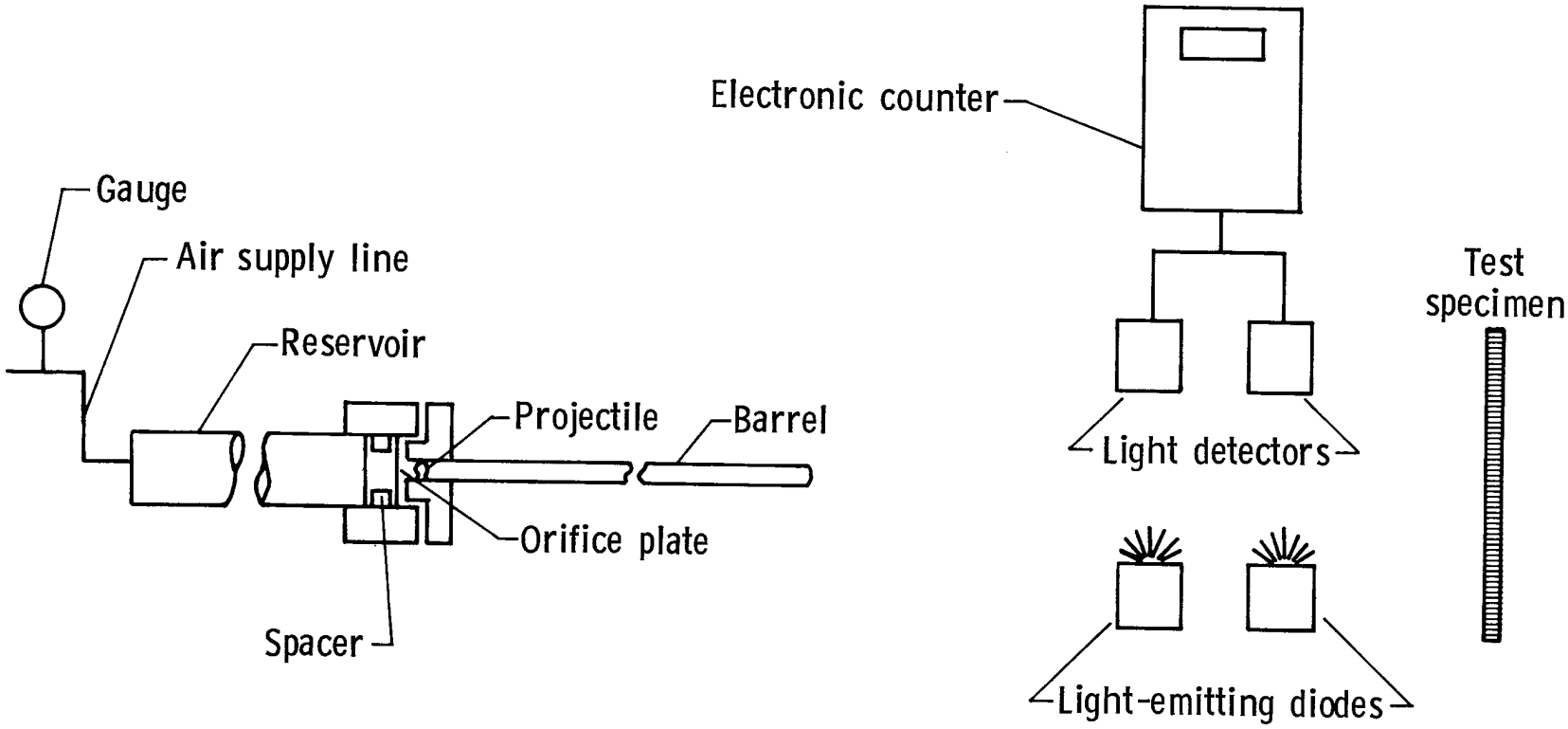

(a) Air-driven impact gun.

(b) Velocity detector.

Figure 4. Schematic diagram of air-driven impact gun and velocity detector.

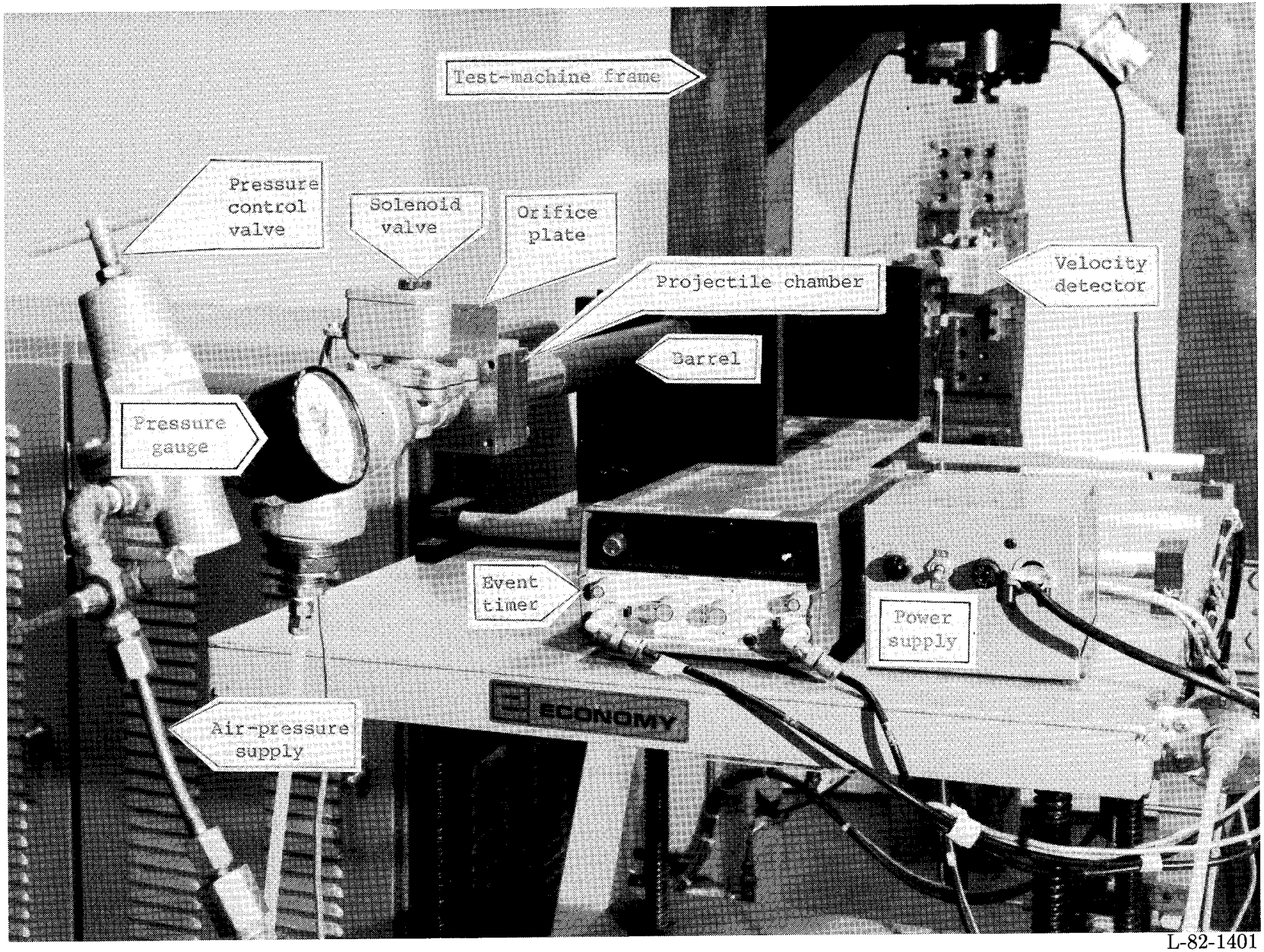

(a) Air-driven impact gun.

Figure 5. Apparatus for impacting plates under load.

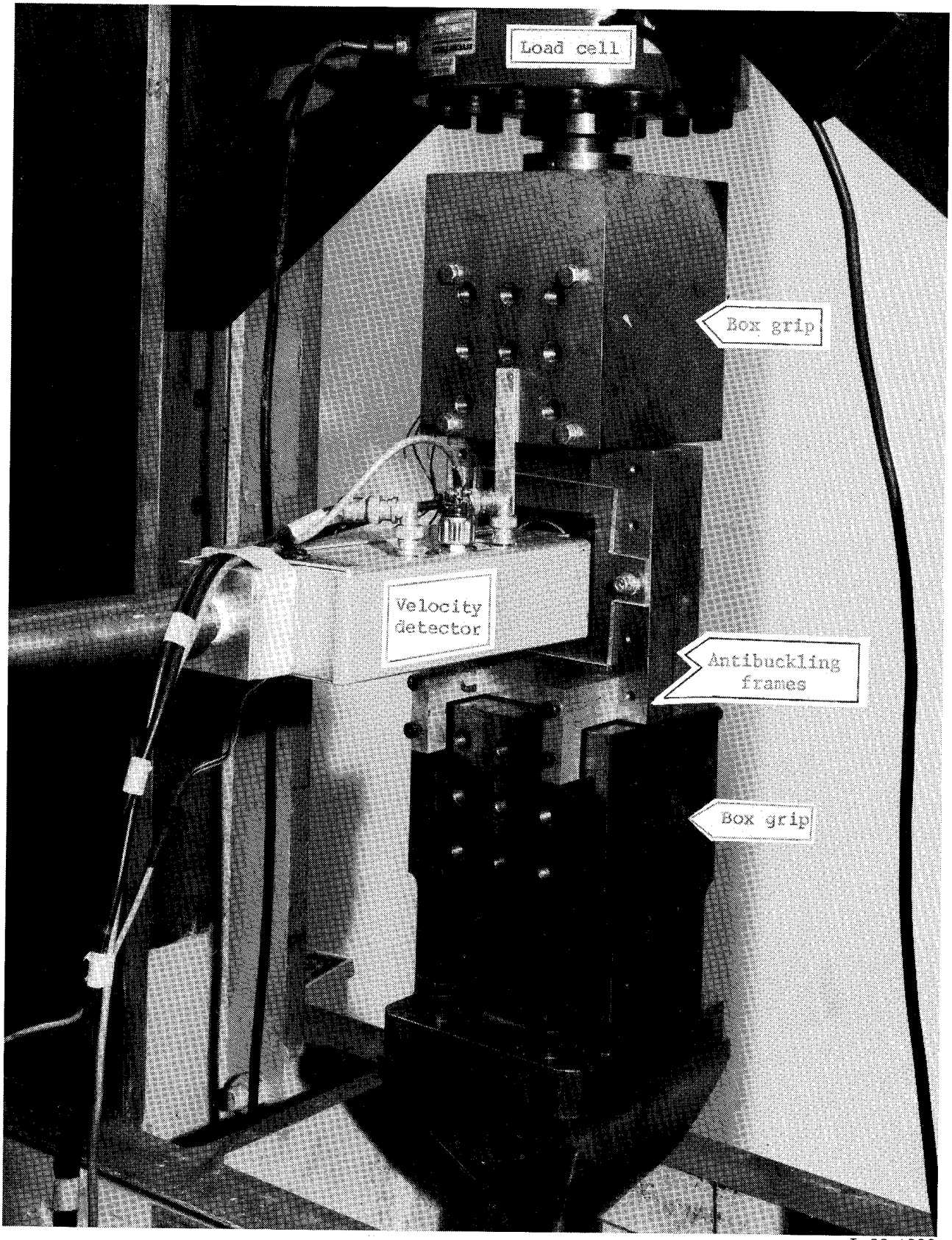

L-82-1399

(b) Velocity detector and load train.

Figure 5. Continued.

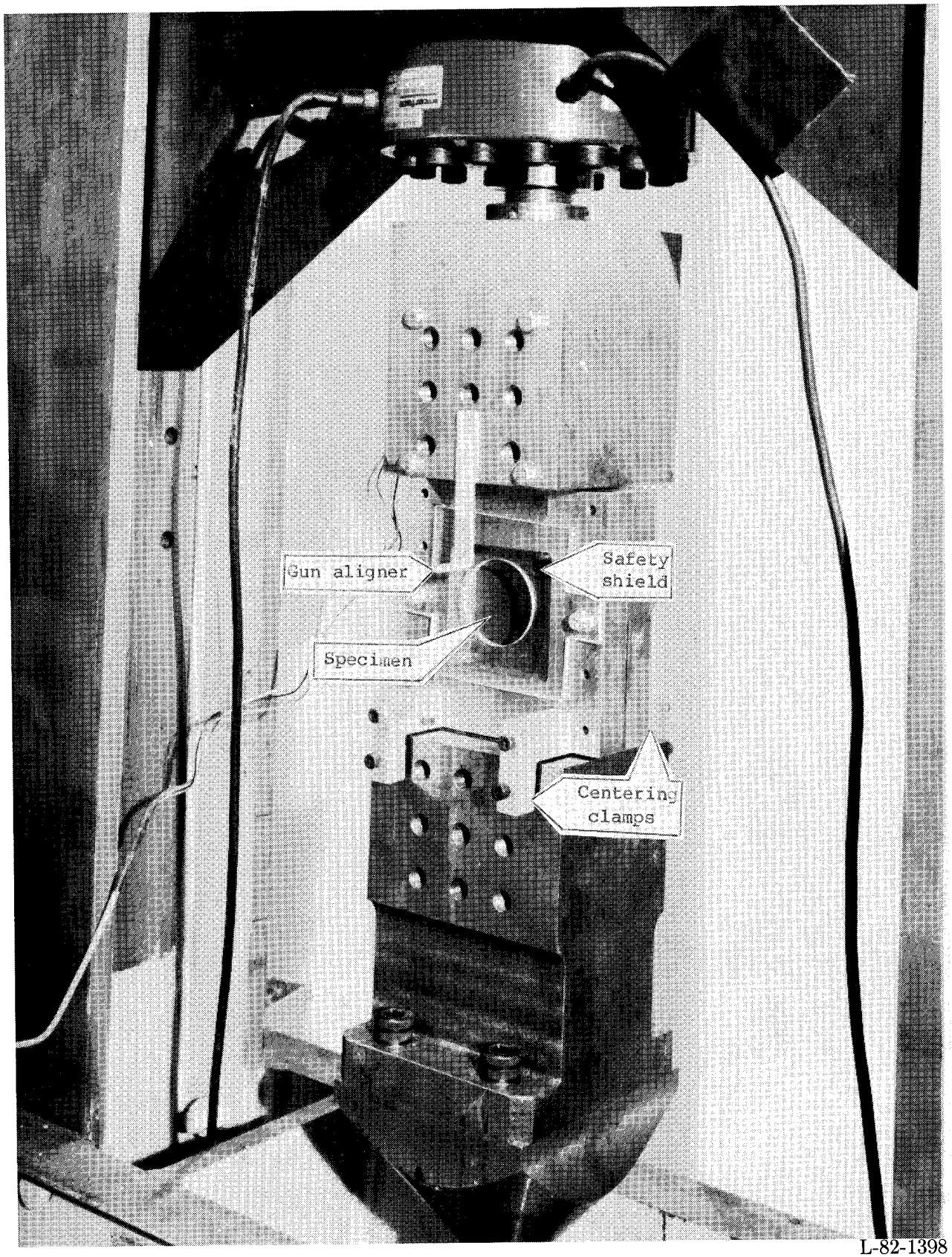

(c) Specimen and load train; impact side.

Figure 5. Continued.

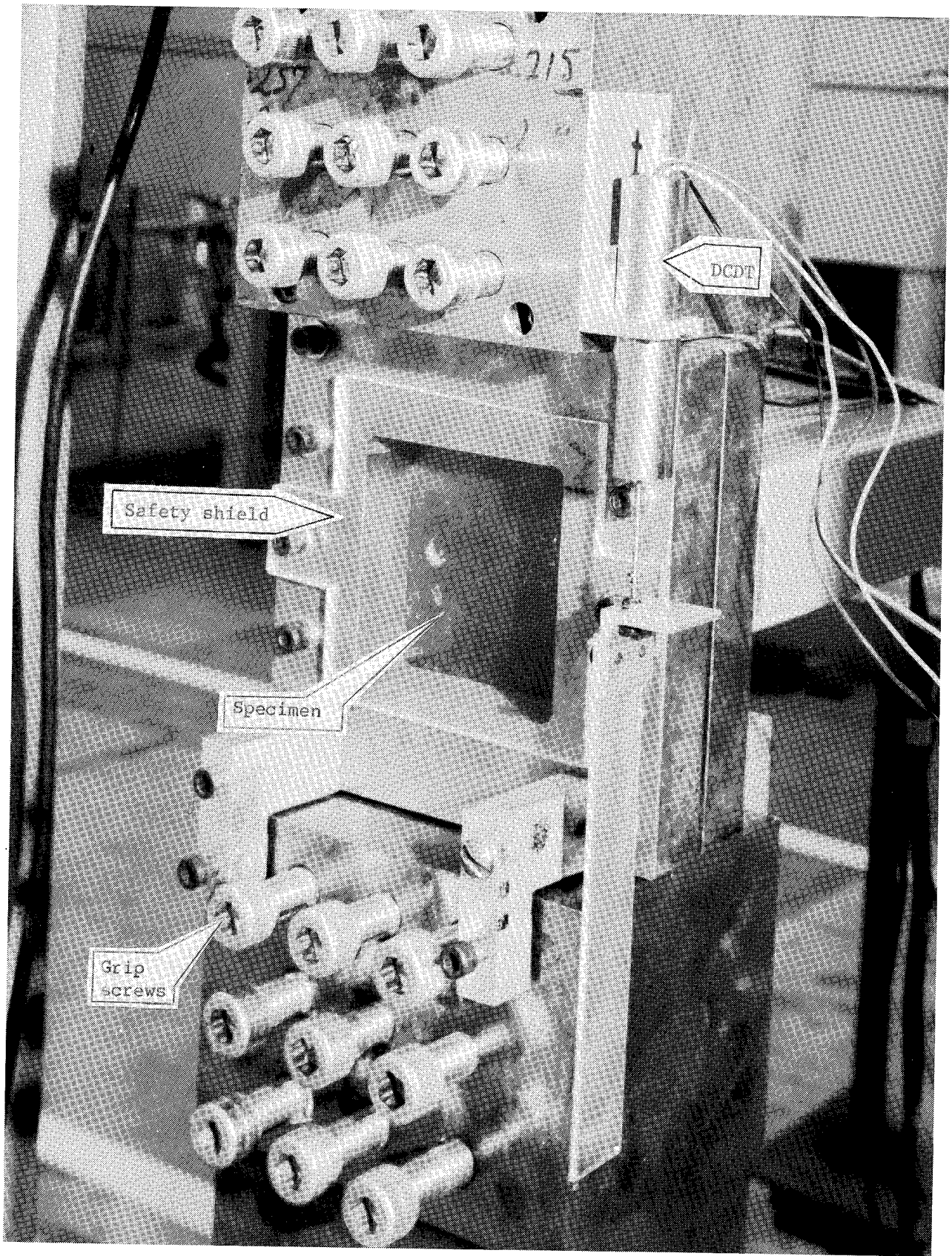

L-82-1397

(d) Specimen and load train; nonimpact side.

Figure 5. Concluded.

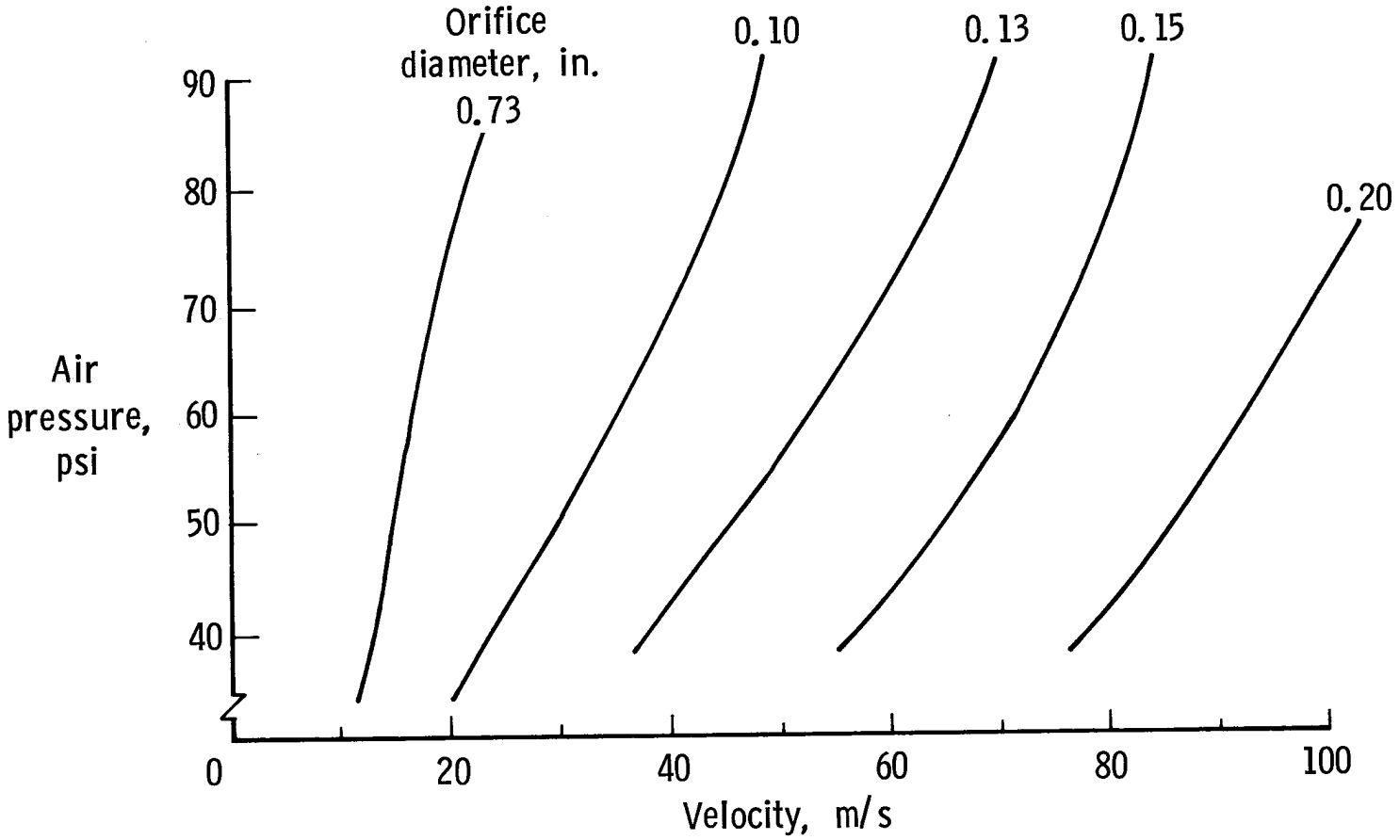

Figure 6. Calibration of air-driven impact gun.

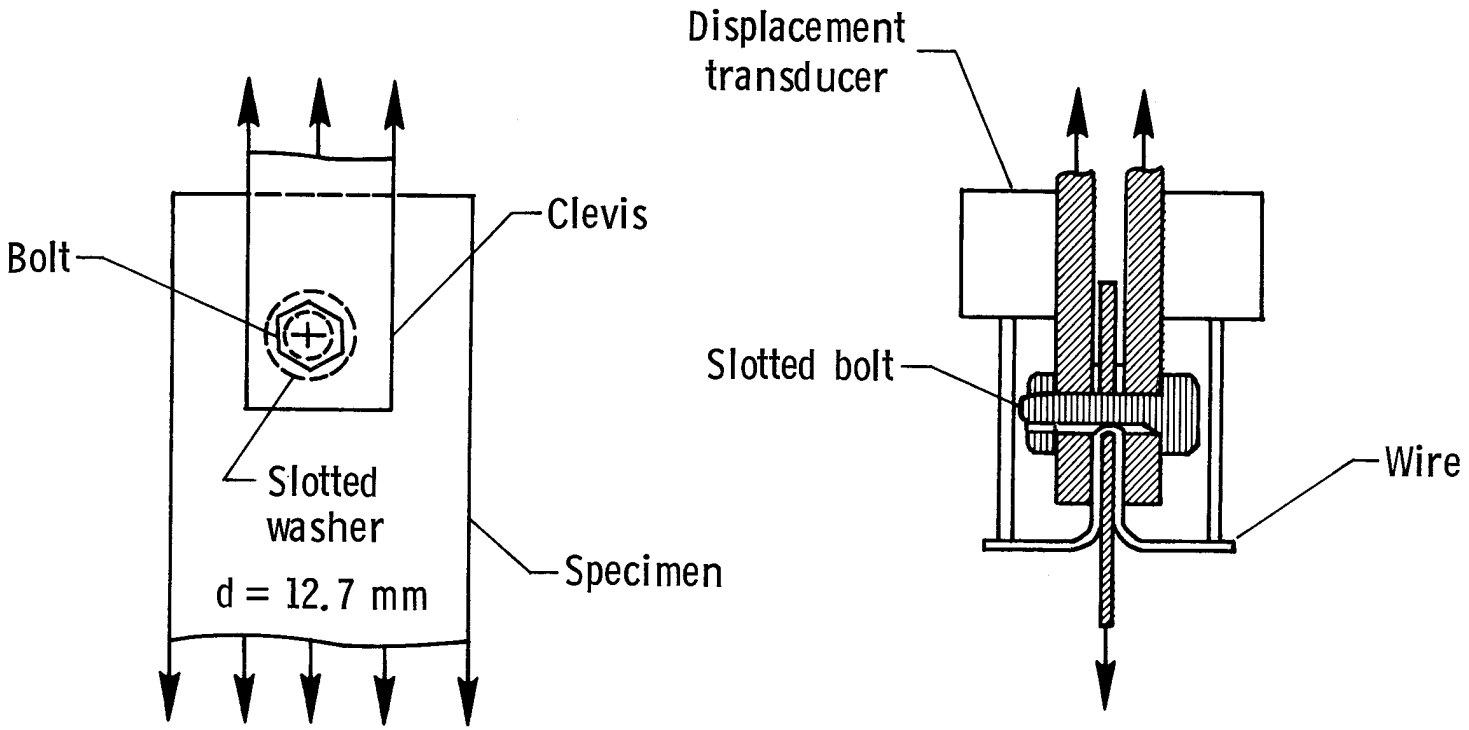

(a) Loading method.

(b) Hole-elongation detector.

Figure 7. Test apparatus for loaded-hole specimens.

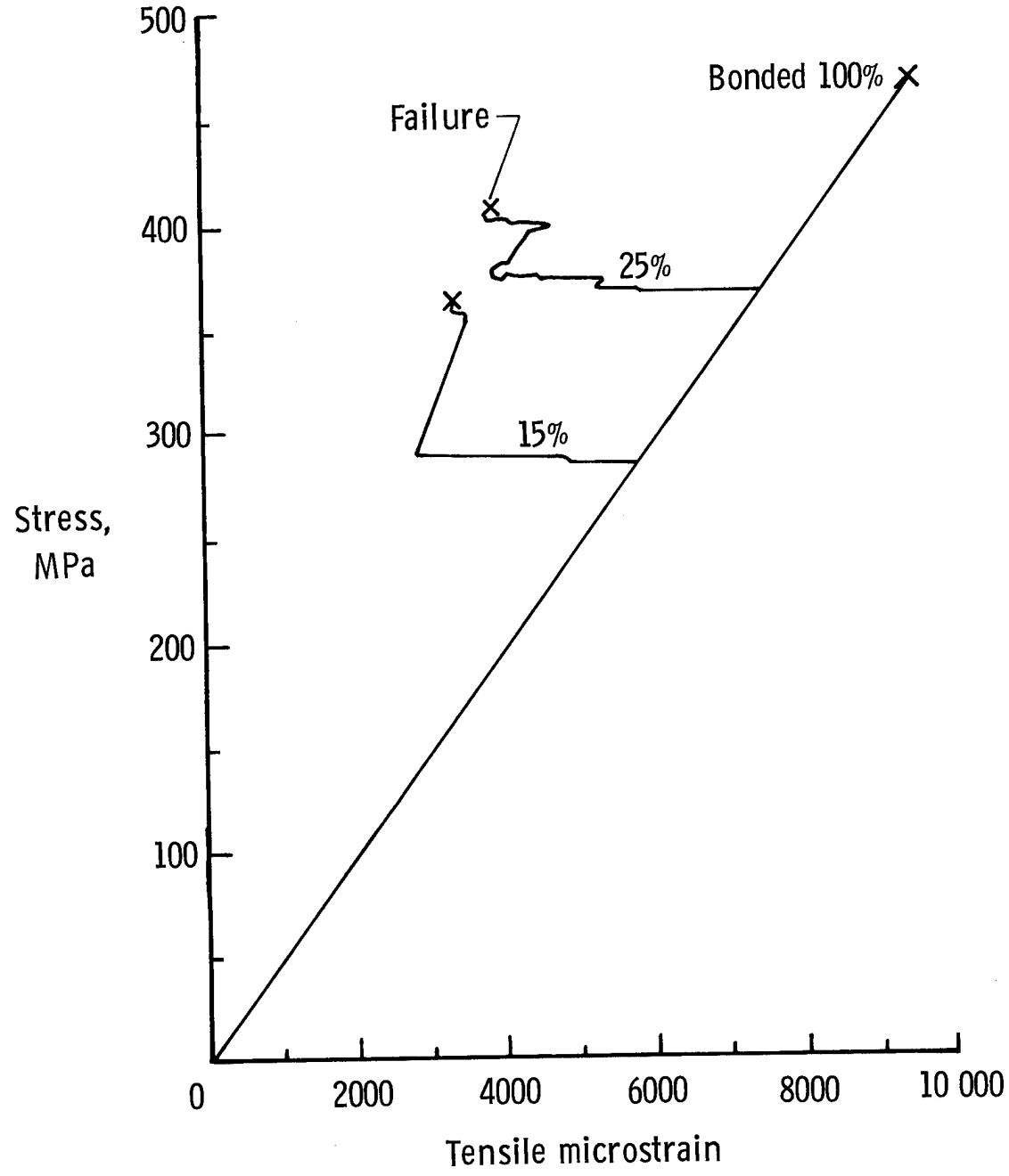

Figure 8. Typical shapes of tensile stress-strain curves.

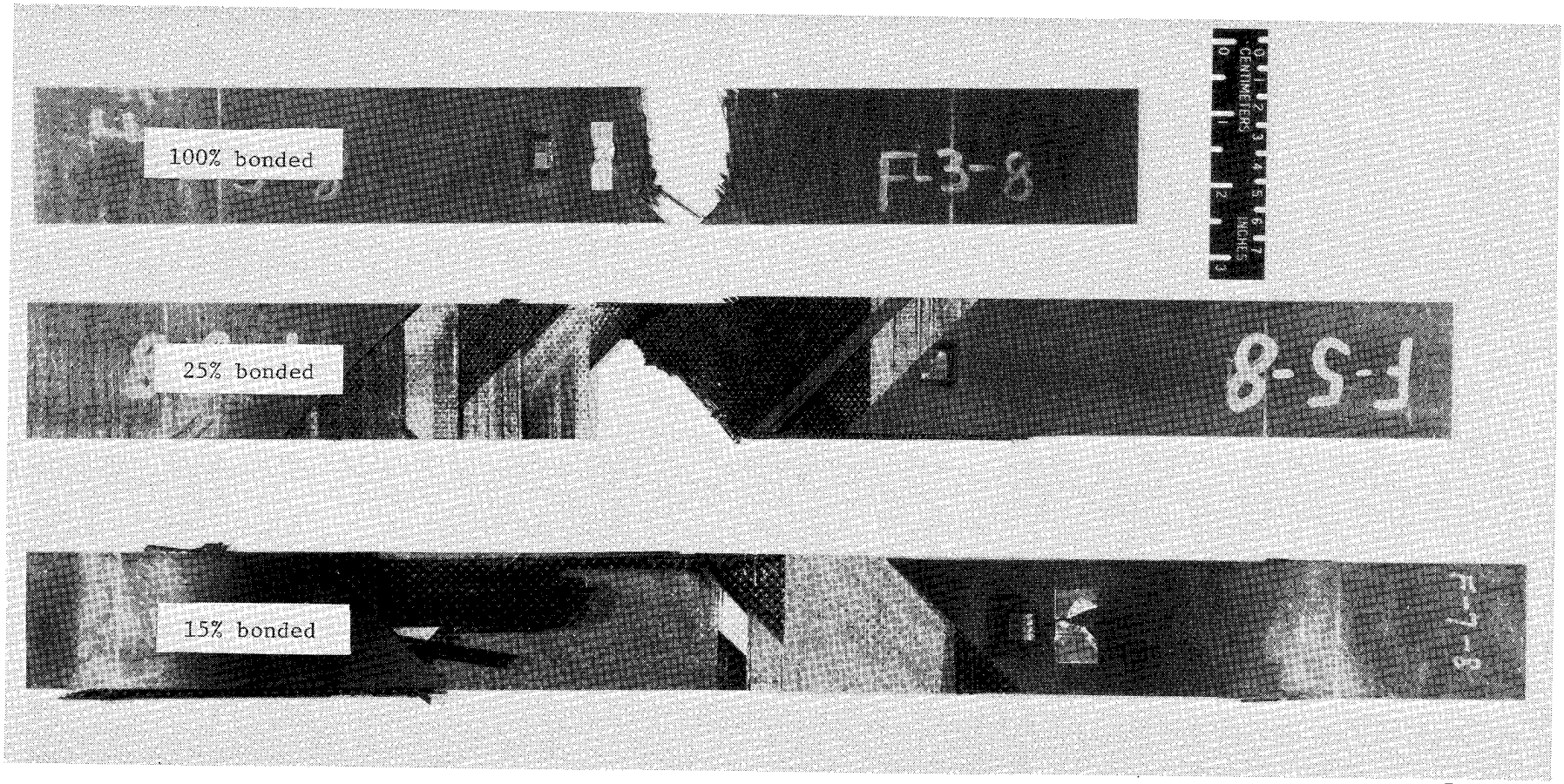

L-82-1311

Figure 9. Typical failures of tensile-test specimens.

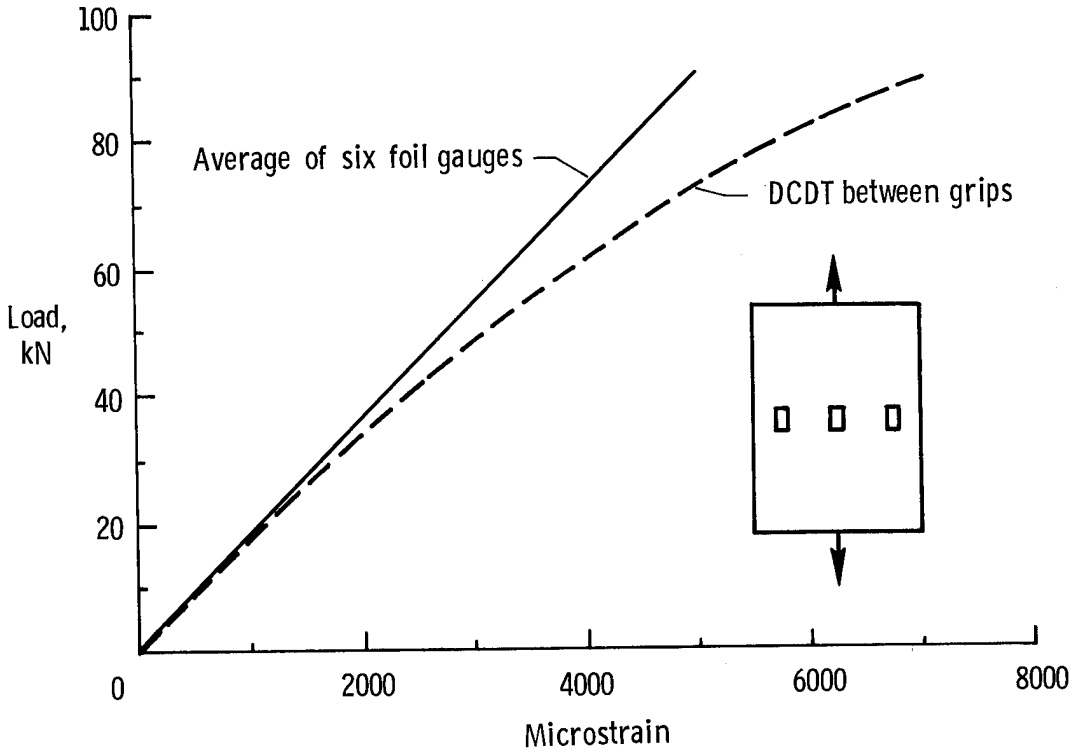

(a) Tension.

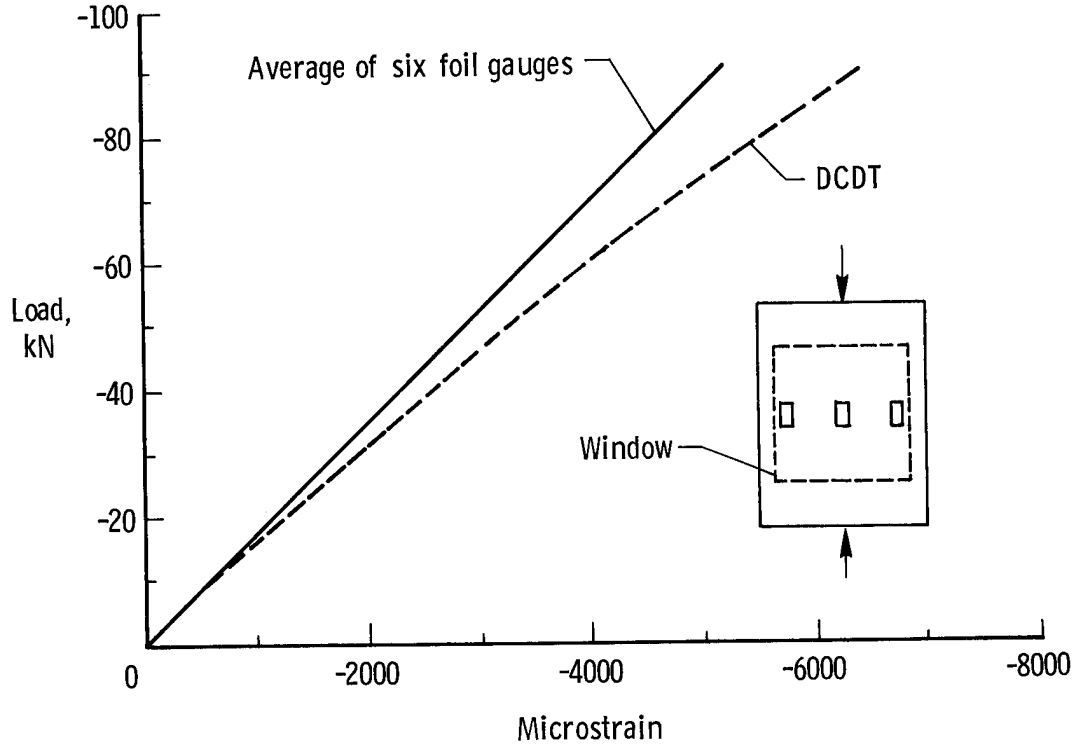

(b) Compression.

Figure 10. Strain determined in two ways: foil gauges and direct-current differential transformer (DCDT).

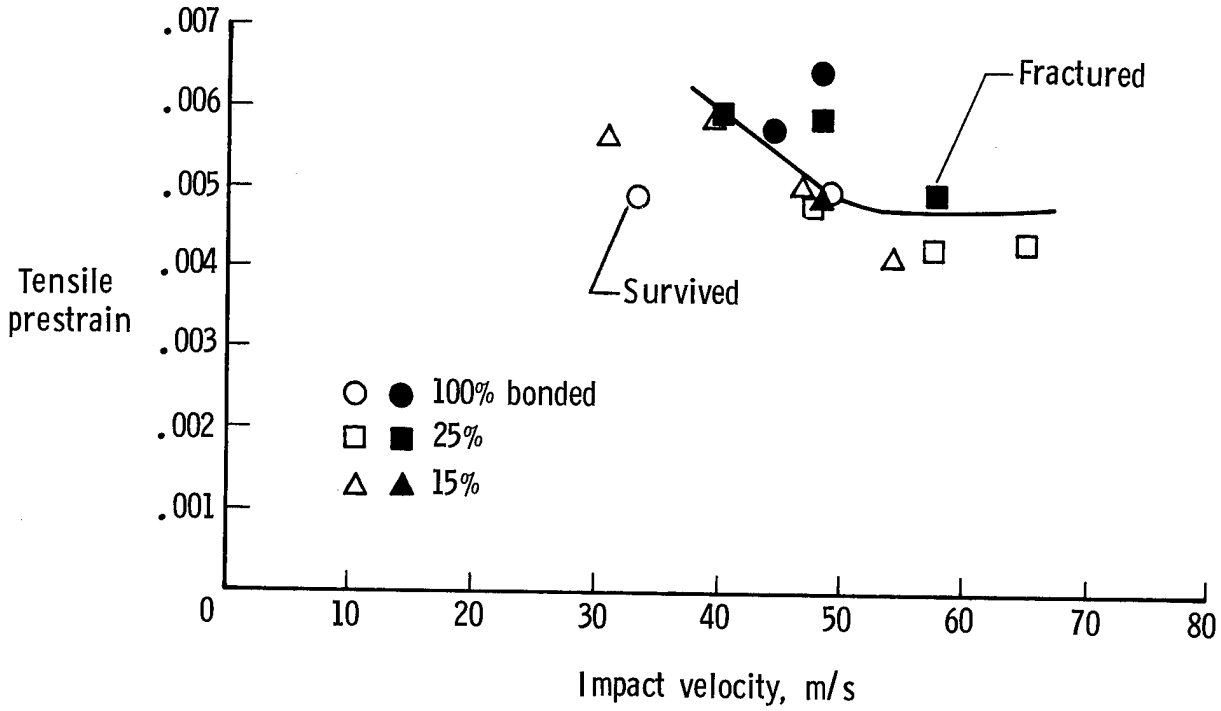

Figure 11. Effect of tensile prestrain and impact velocity on threshold curve for fracture. T300/5208; 24 plies.

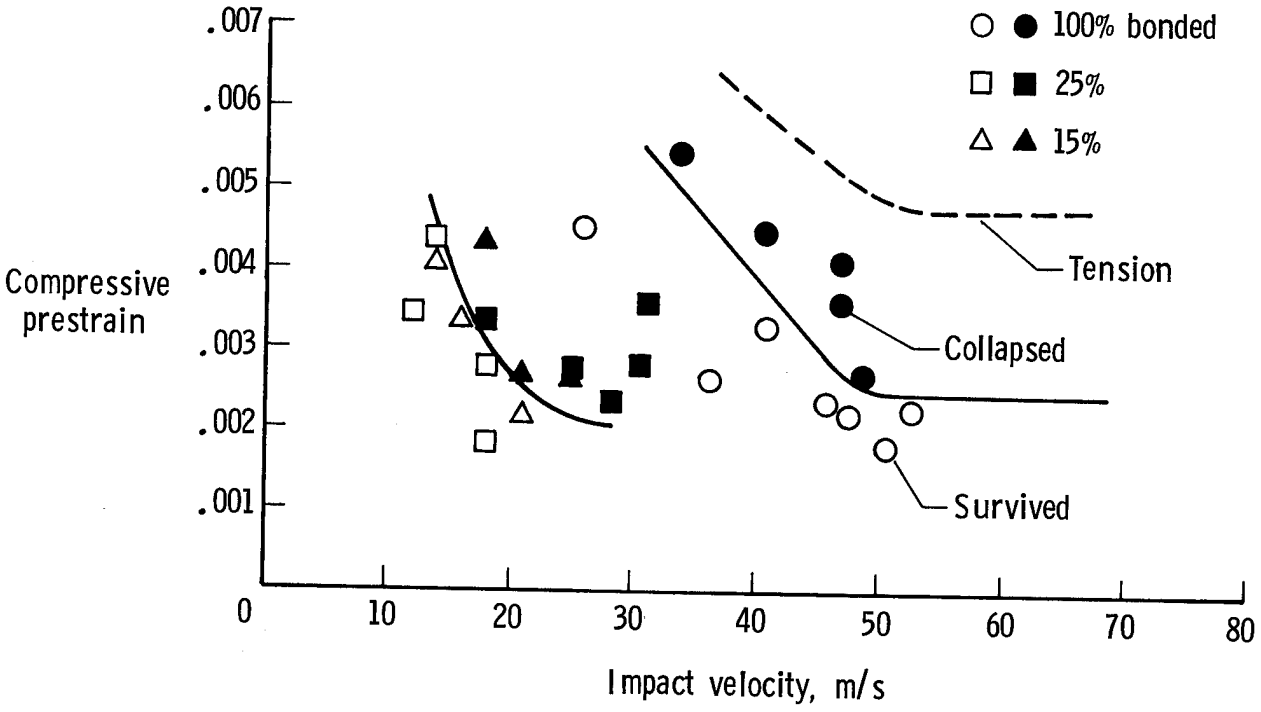

Figure 12. Effect of compressive prestrain and impact velocity on threshold curve for collapse. T300/5208; 24 plies.

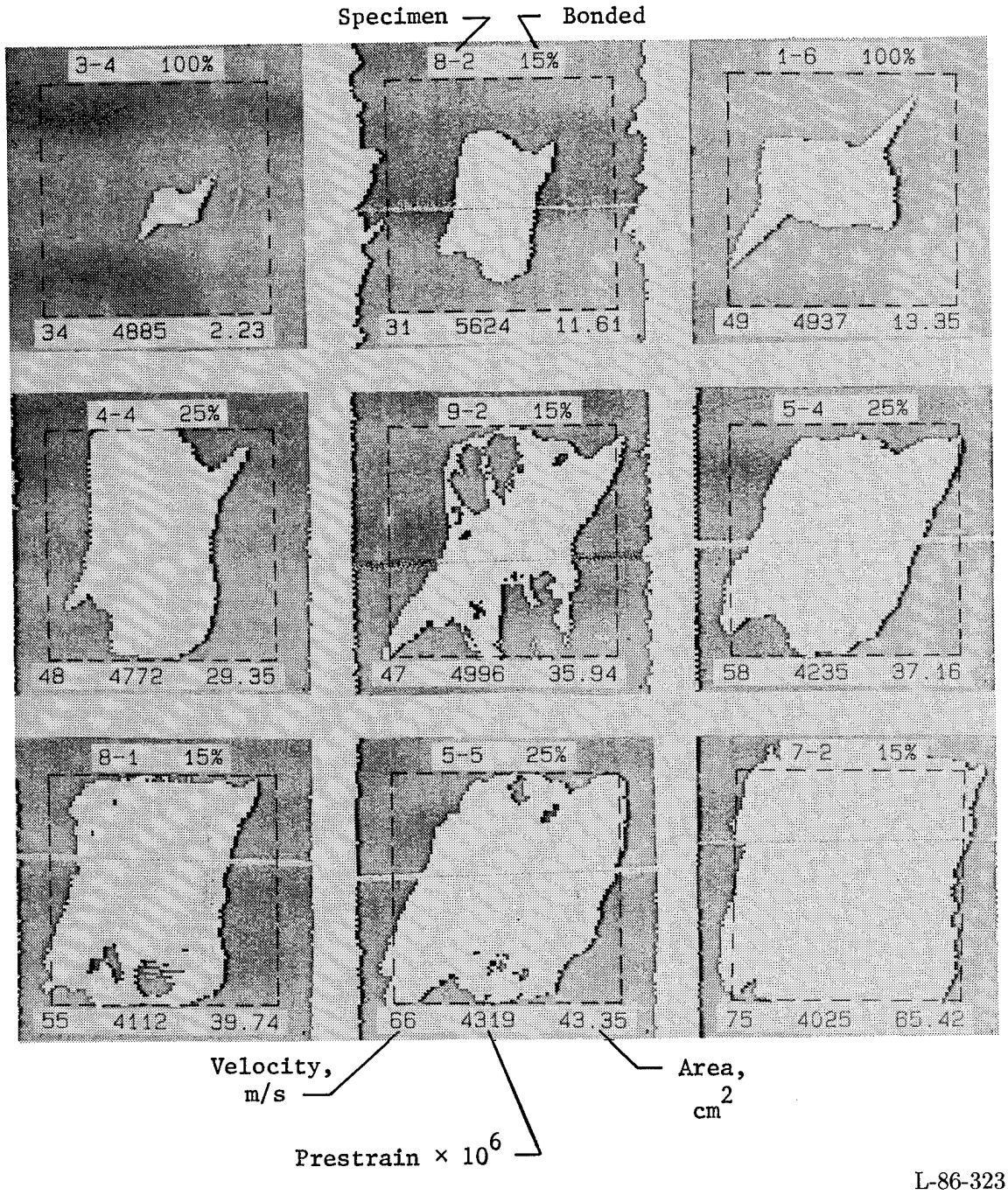

(a) Tensile prestrain.

Figure 13. C-scan of specimens that survived impact while under prestrain. White areas are 6 dB below dark areas; frequency, 10 MHz.

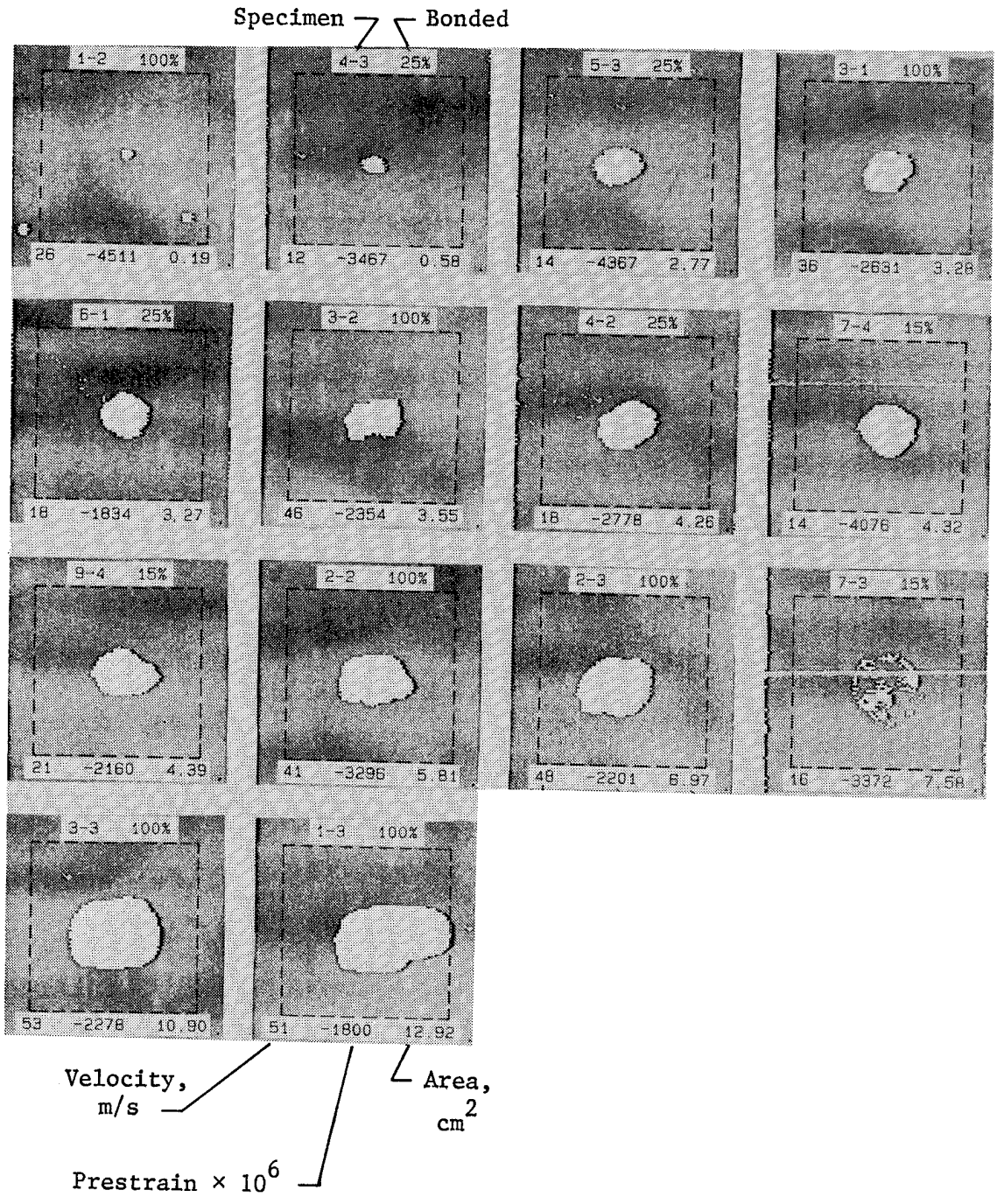

L-86-324

(b) Compressive prestrain.

Figure 13. Concluded.

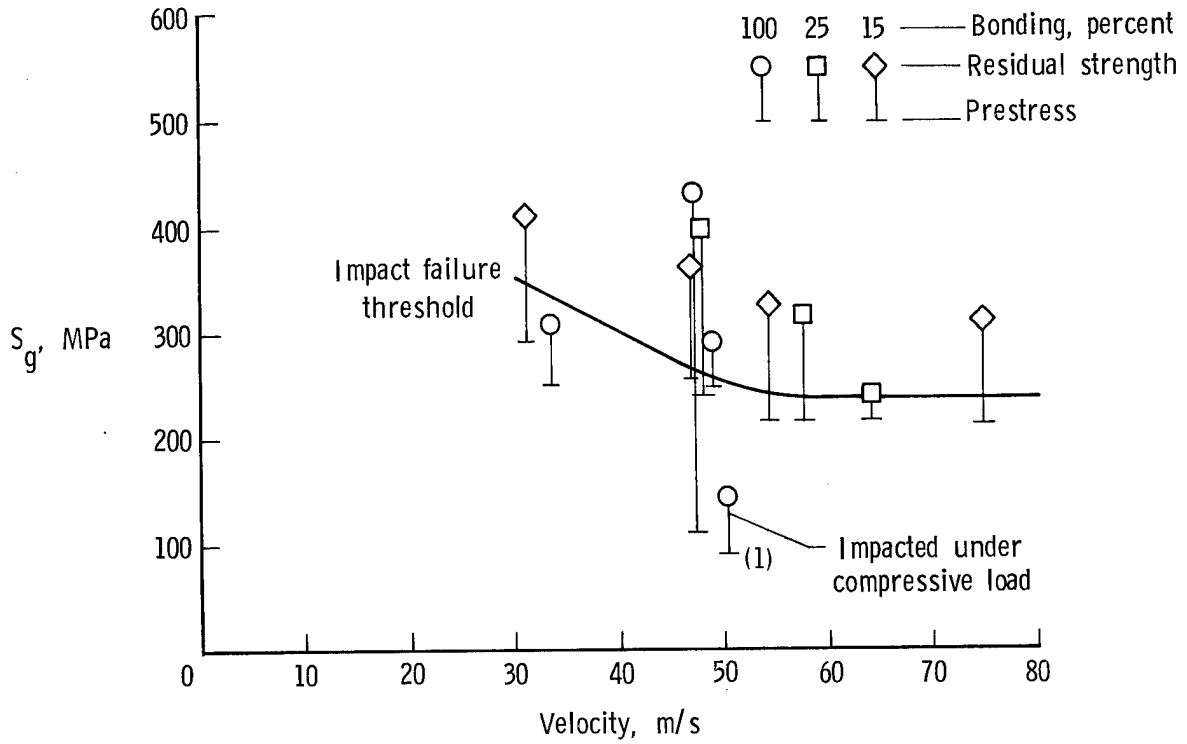

(a) Tension.

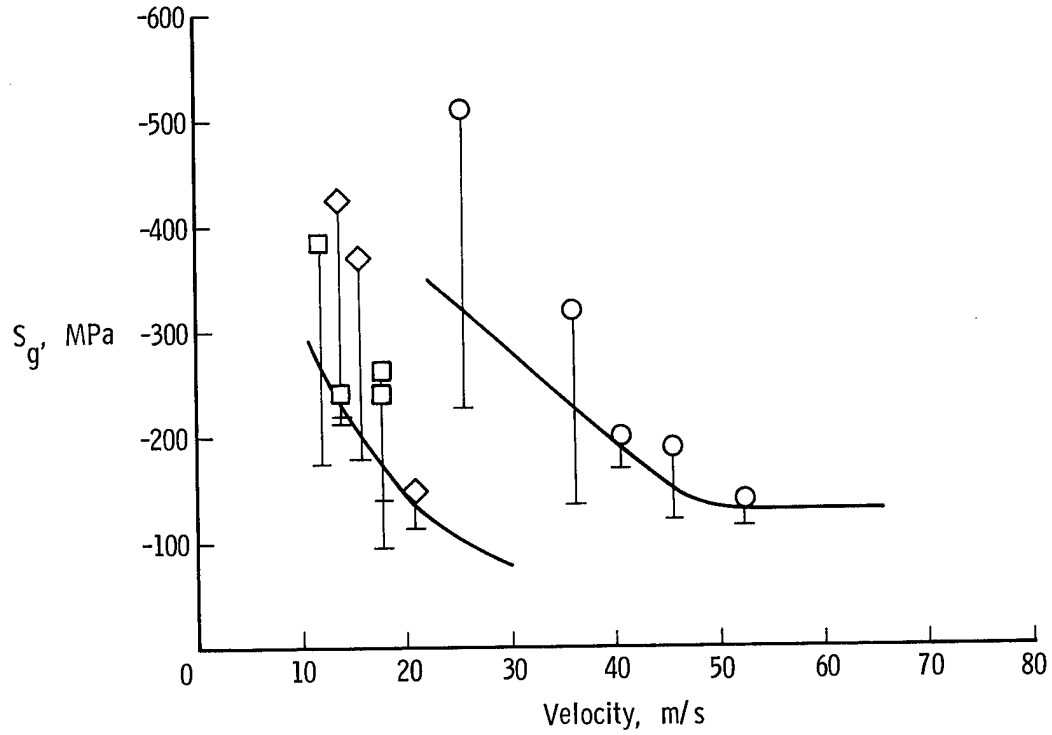

(b) Compression.

Figure 14. Relation of residual strength to threshold for impact failure.

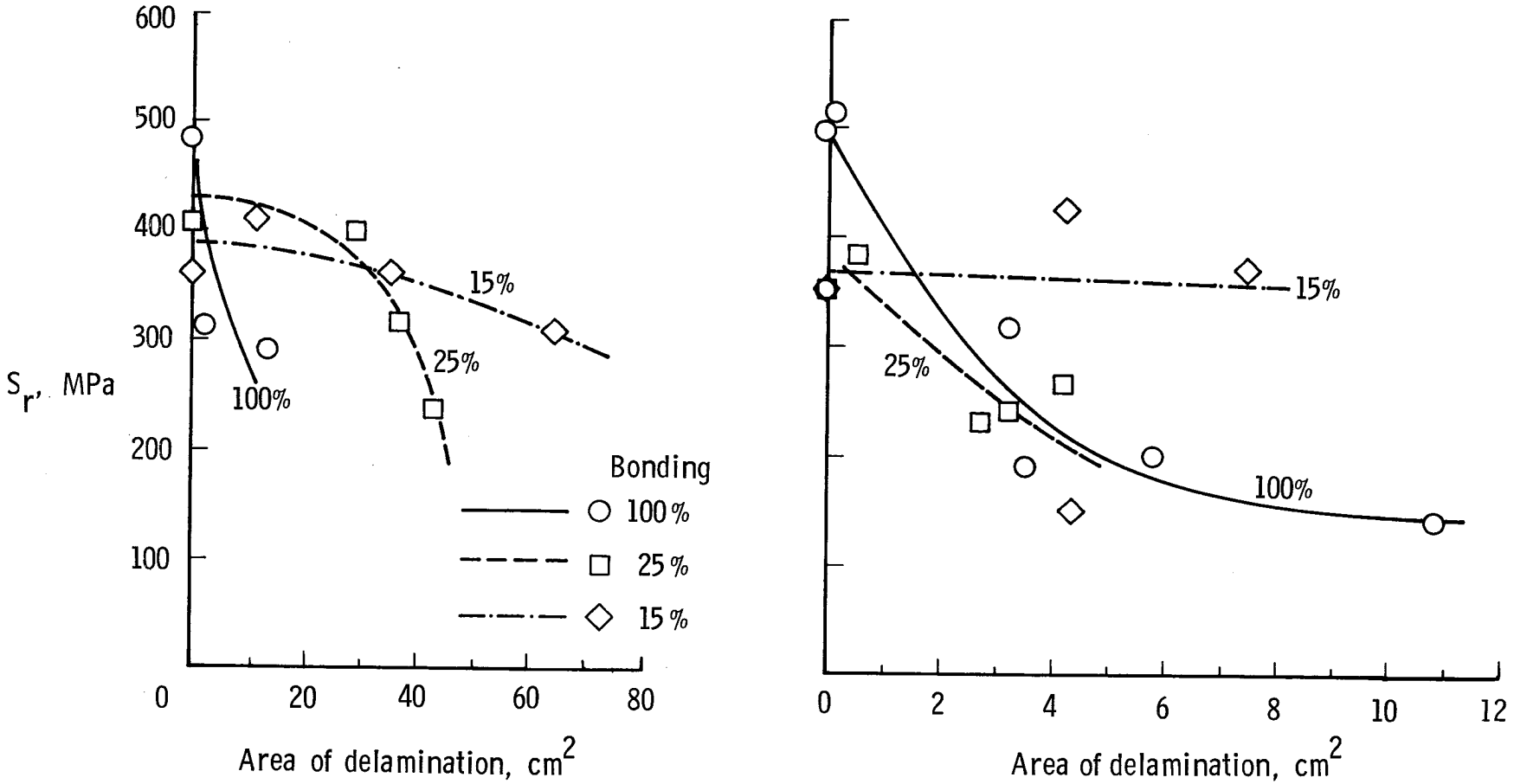

(a) Tension.

(b) Compression.

Figure 15. Residual strength of impact survivors plotted against C-scan area of delamination.

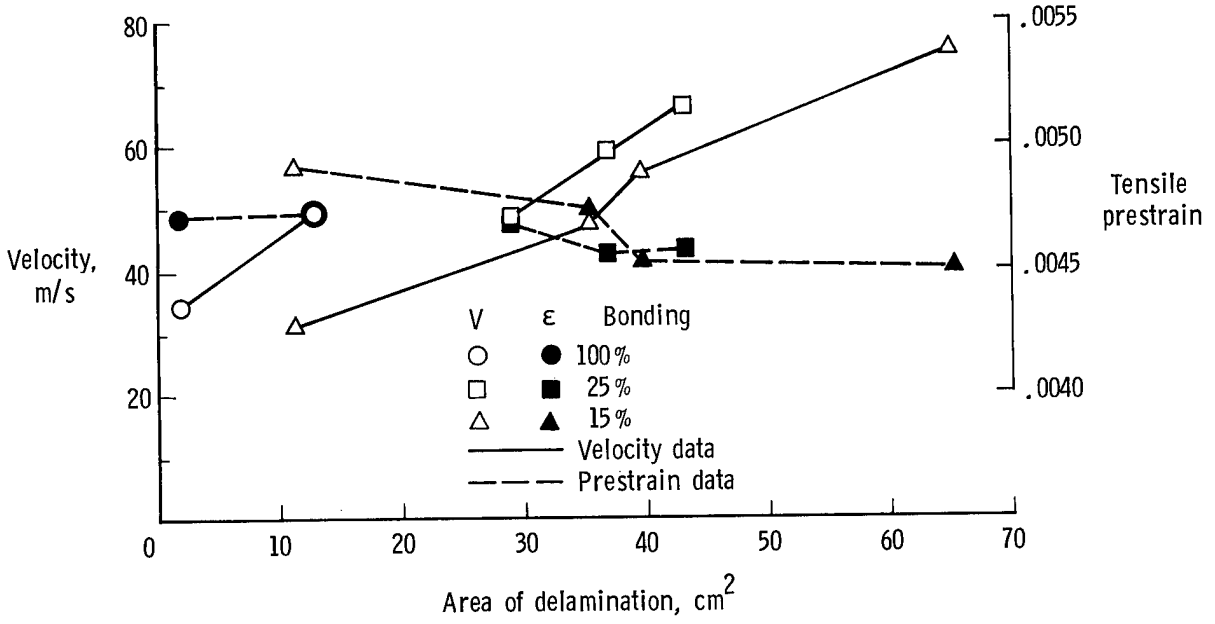

(a) Tensile prestrain.

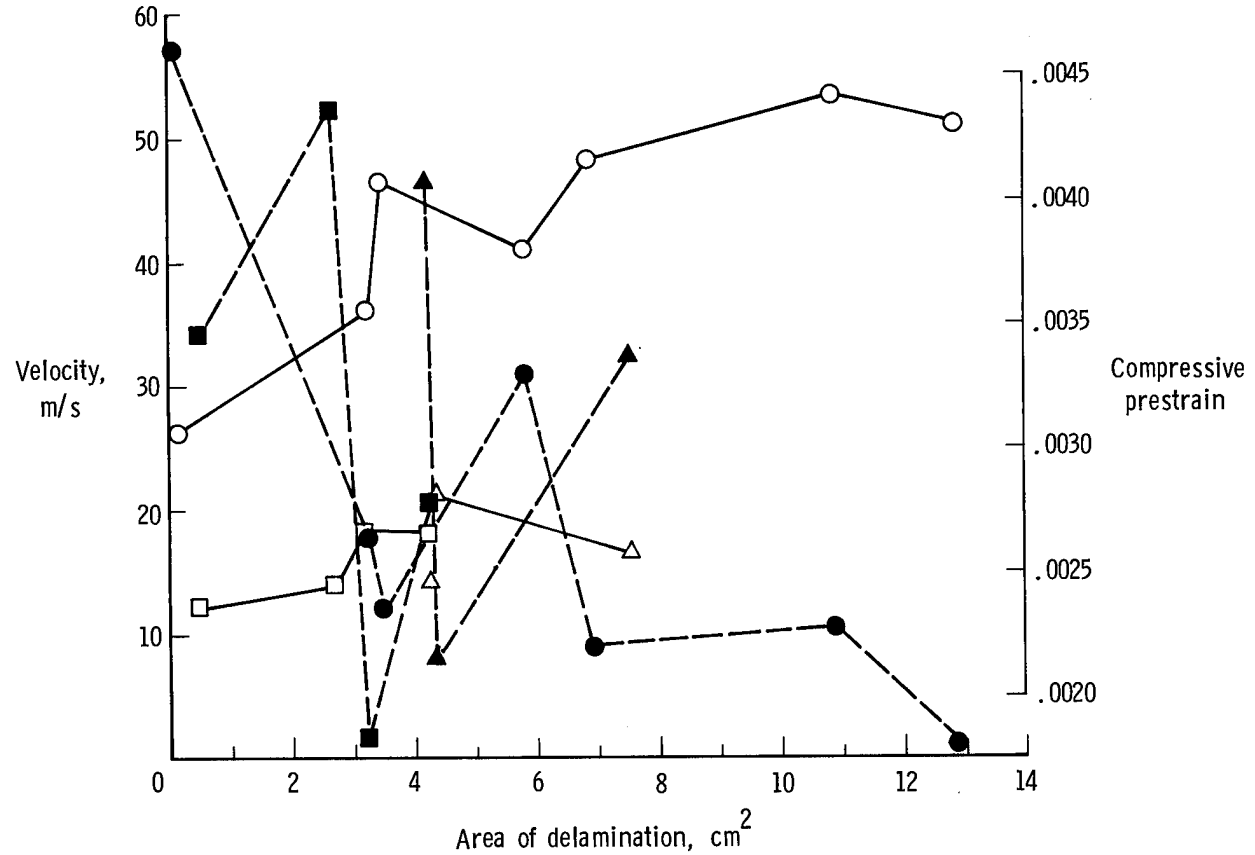

(b) Compressive prestrain.

Figure 16. Combined effects of velocity and prestrain on area of delamination.

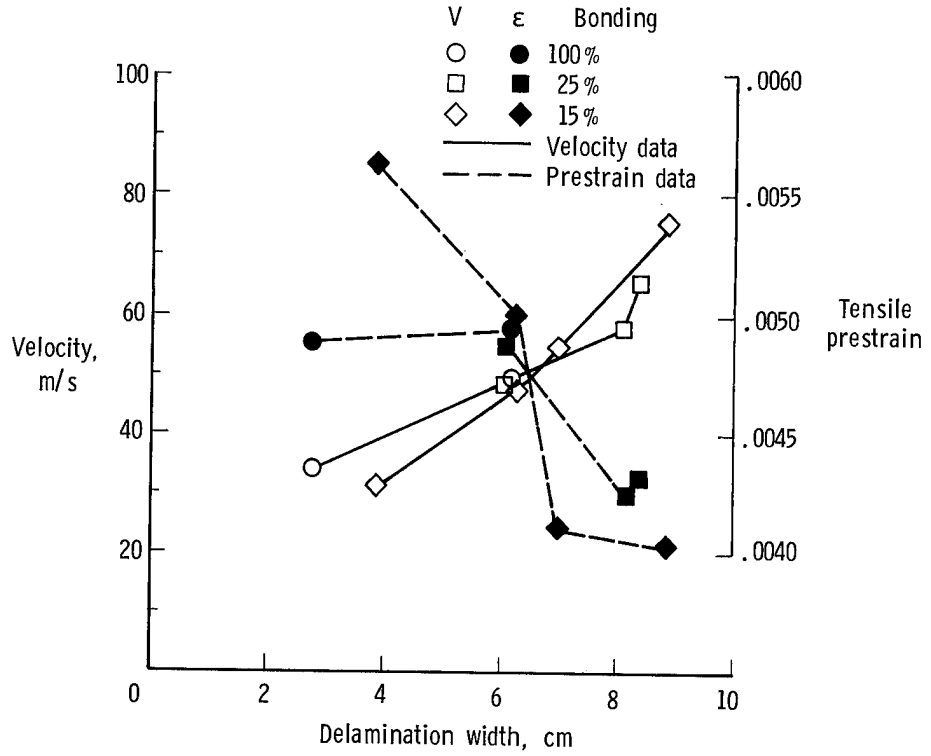

(a) Tensile prestrain.

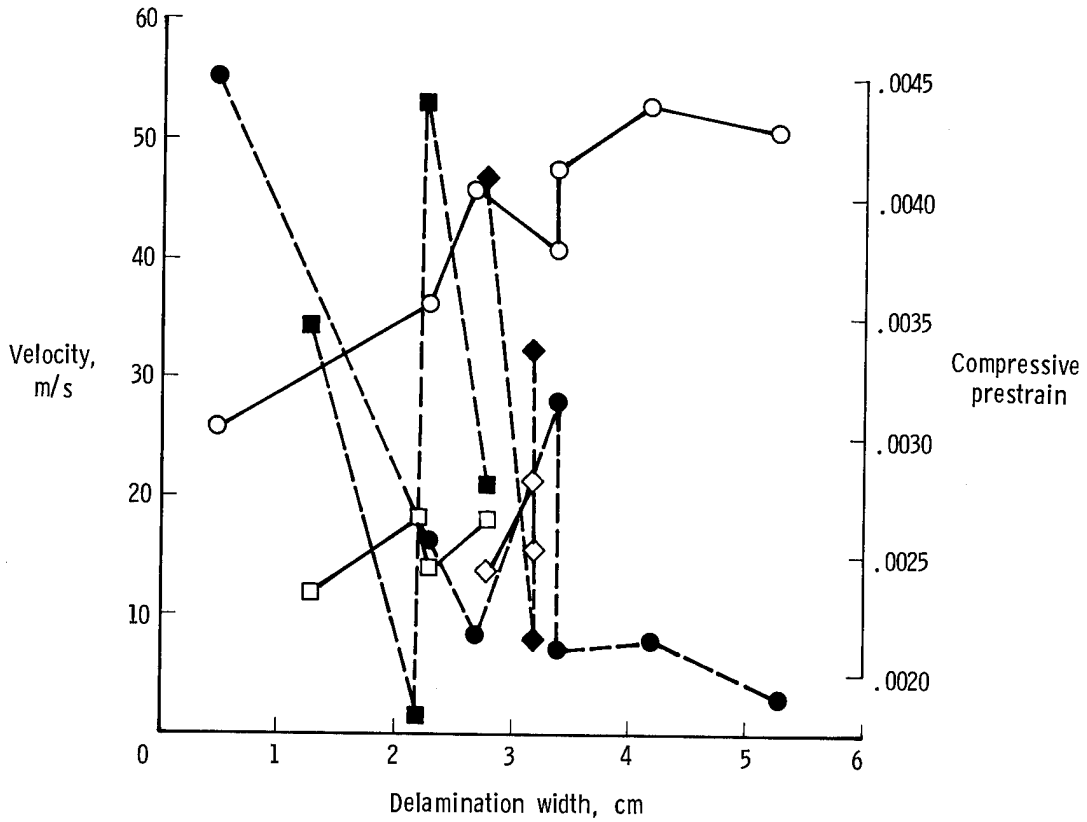

(b) Compressive prestrain.

Figure 17. Combined effect of velocity and prestrain on delamination width.

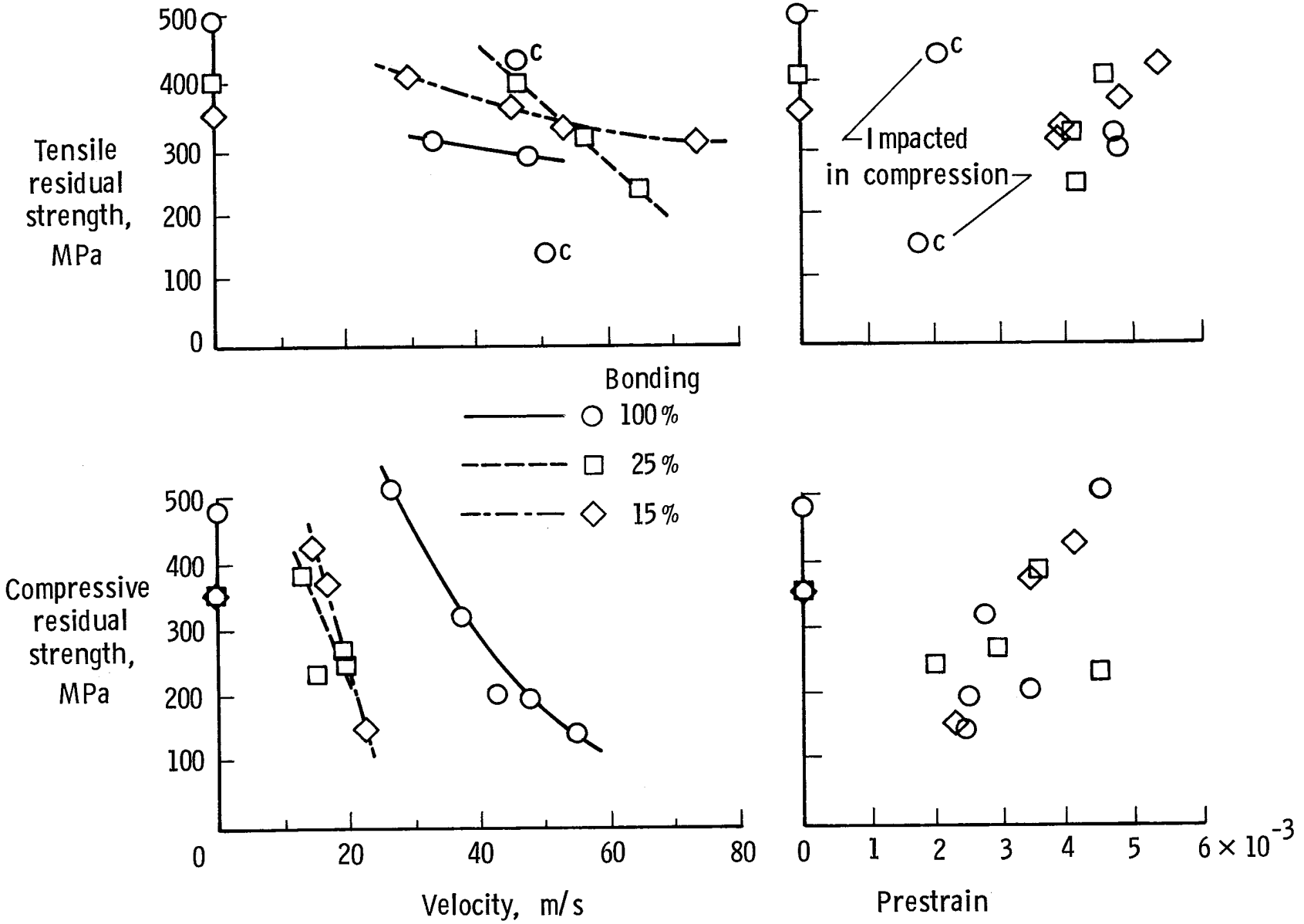

Figure 18. Correlations of residual strength with velocity and prestrain.

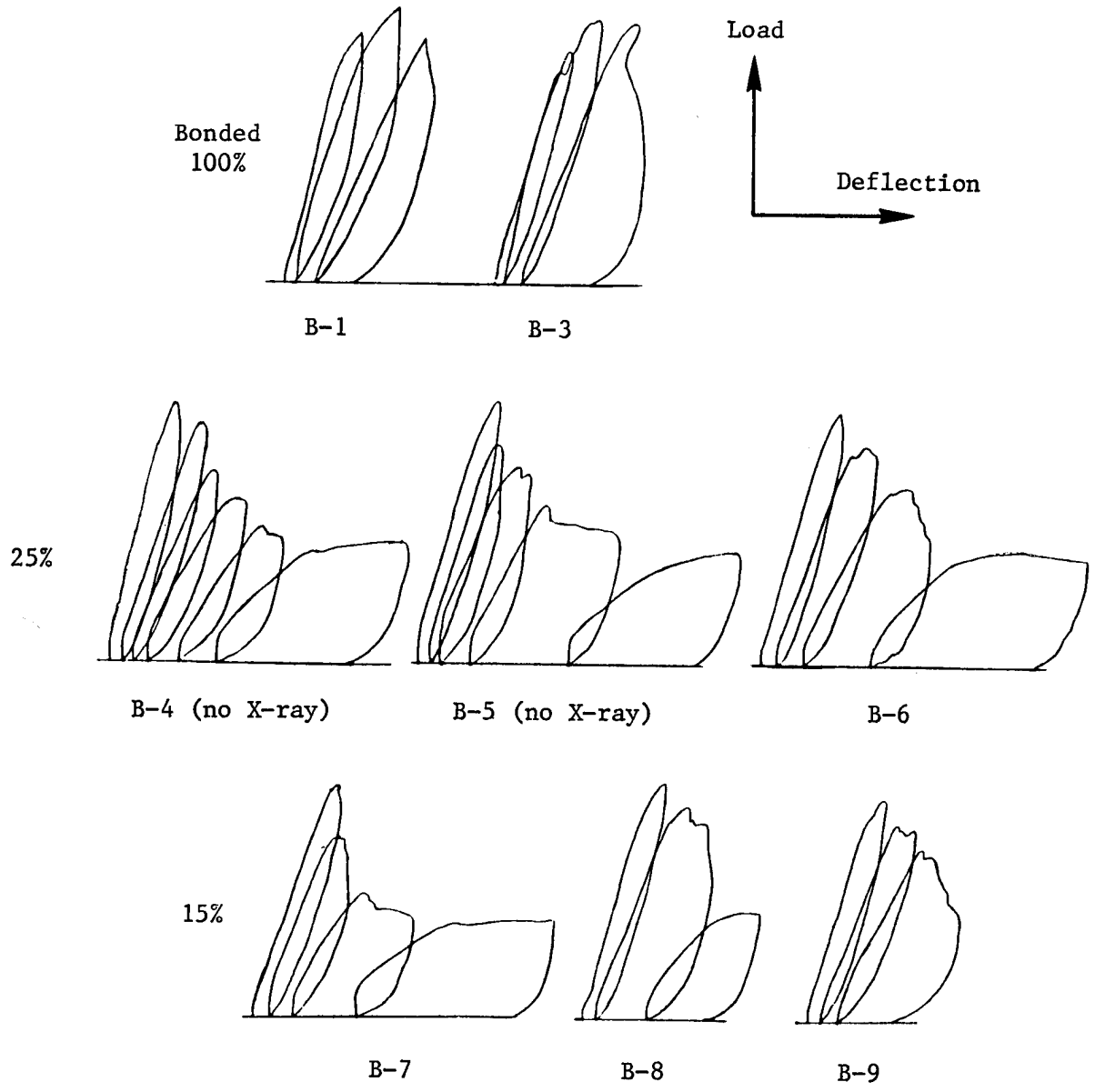

(a) Bearing critical; none failed.

Figure 19. Traces of load-deflection curves for loaded-hole specimens.

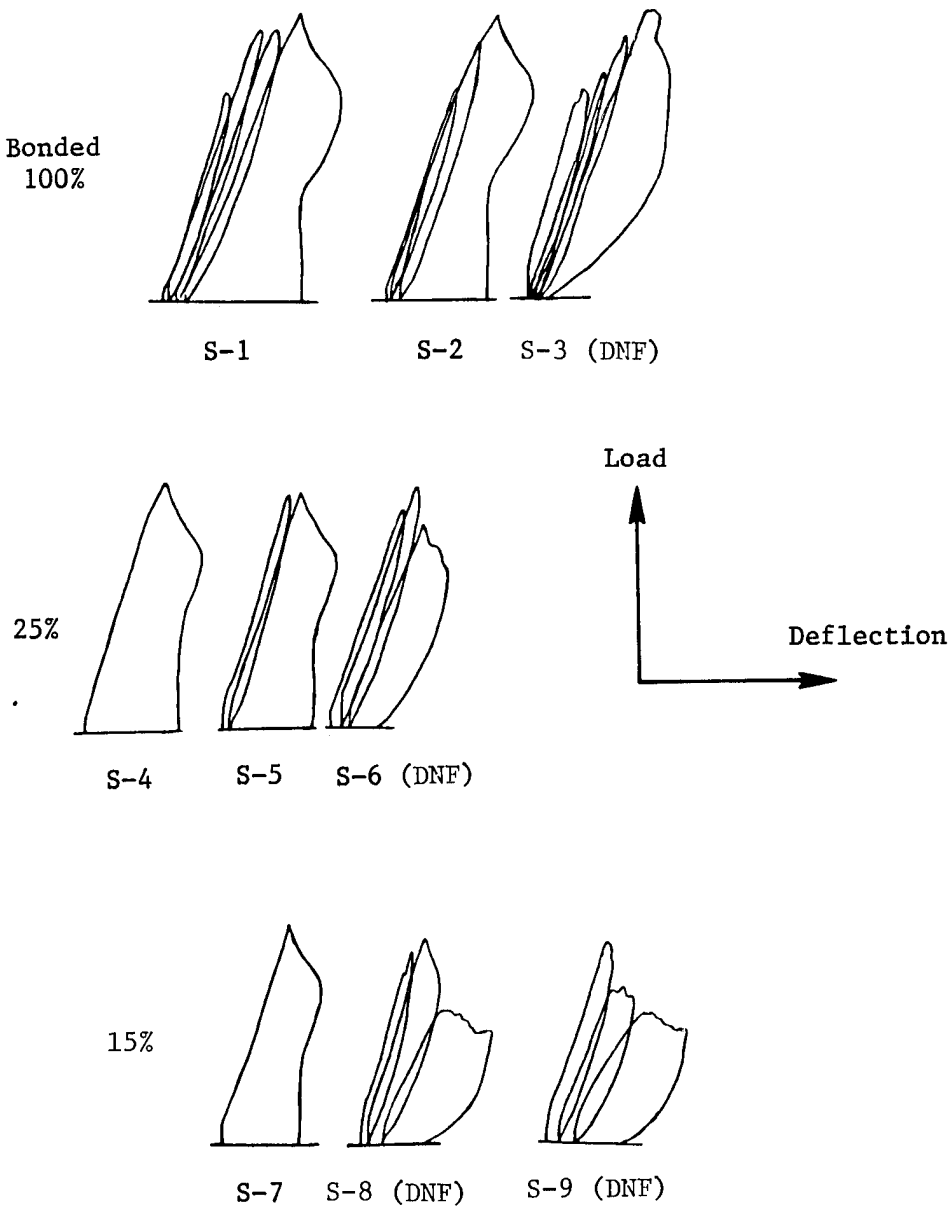

(b) Shear critical; DNF denotes specimens that did not fail.

Figure 19. Continued.

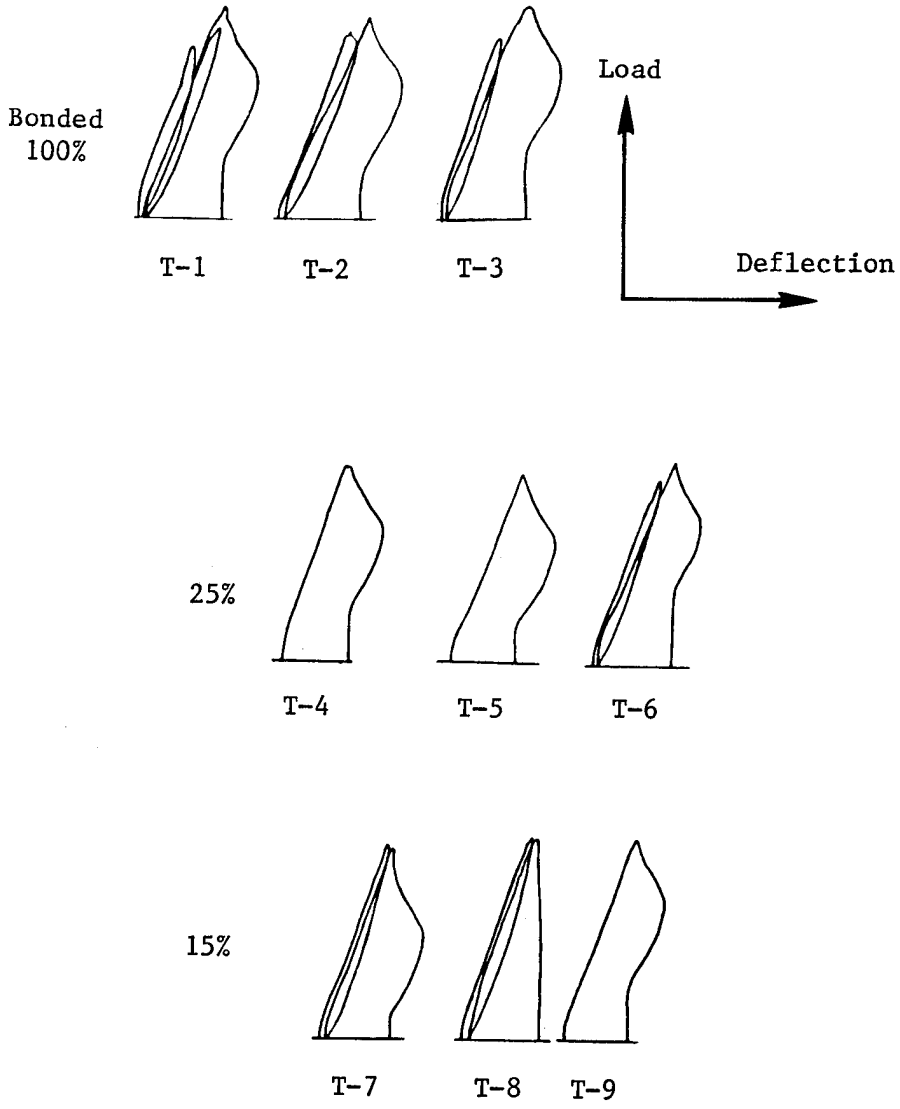

(c) Tension critical; all failed.

Figure 19. Concluded.

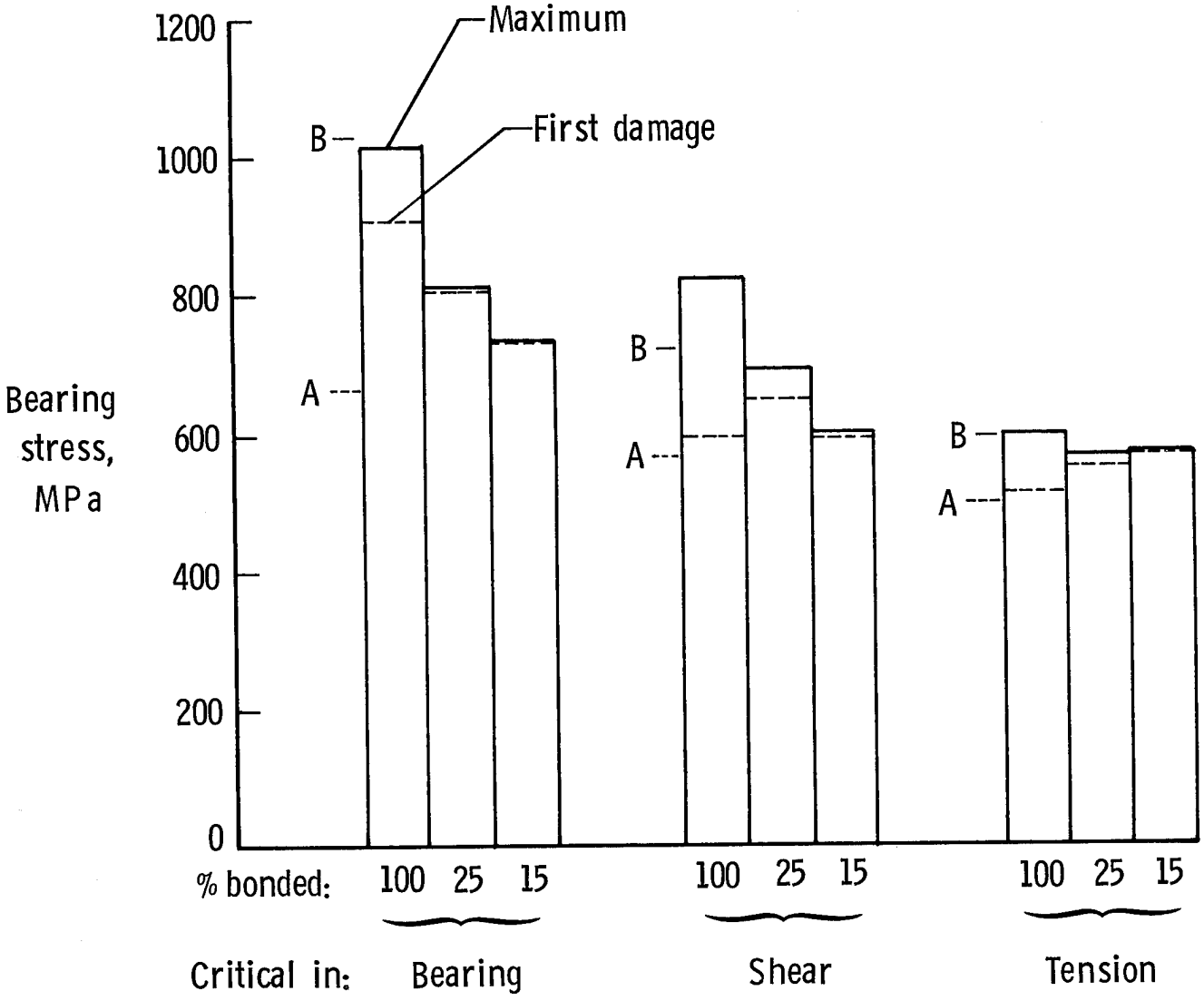

Figure 20. Effect of partial bonding on maximum bearing stress S_b. Points A and B denote first-damage stress and maximum stress, respectively, for 16-ply laminates in reference 15.

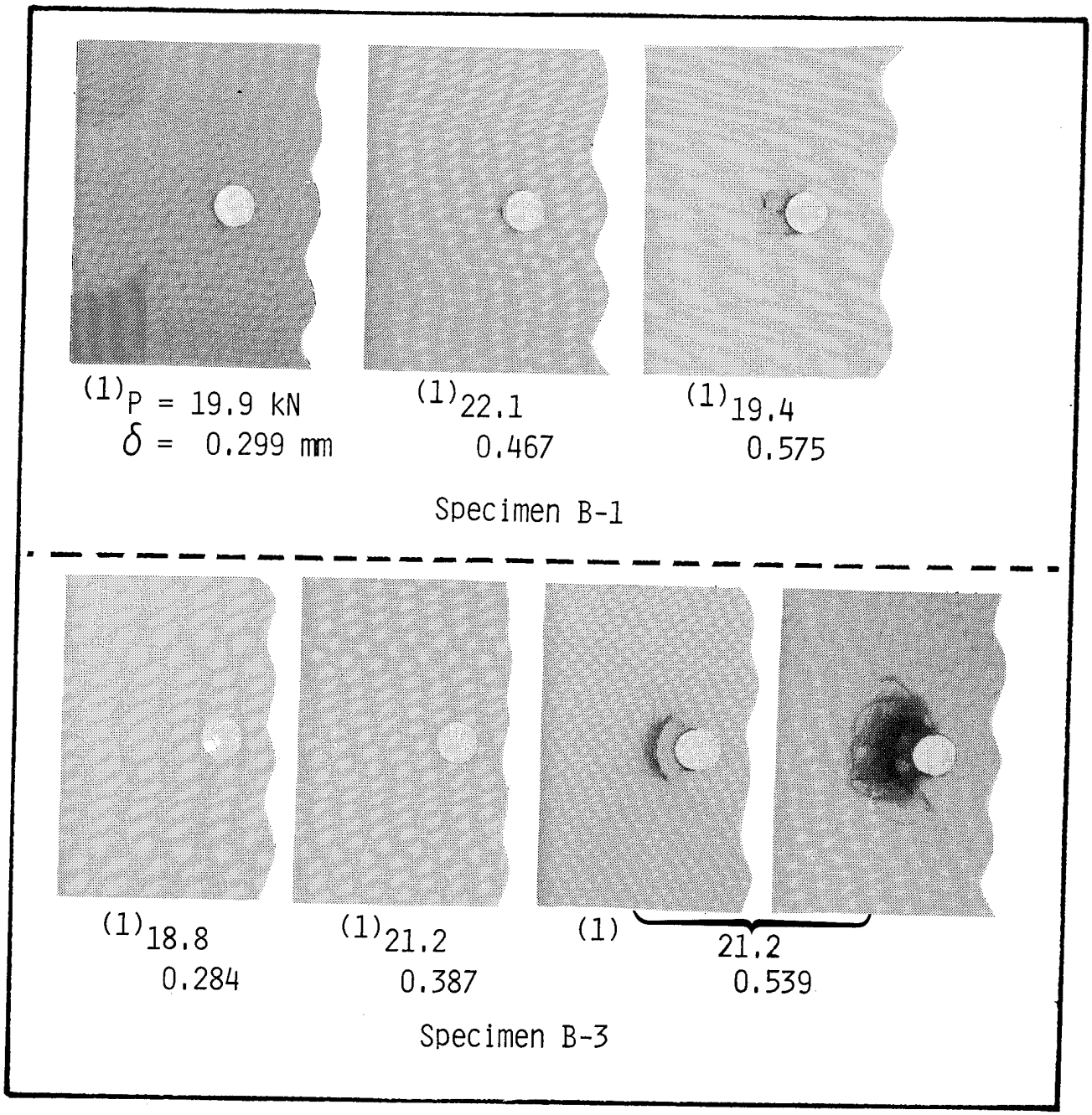

(1)Gold chloride used in place of zinc iodide.

L-86-325

(a) 100-percent bonded. Gold chloride used as enhancer except for final view of specimen B-3.

Figure 21. Radiographs of bearing-critical specimens. Pin loaded toward left; zinc iodide was used as enhancer unless otherwise noted.

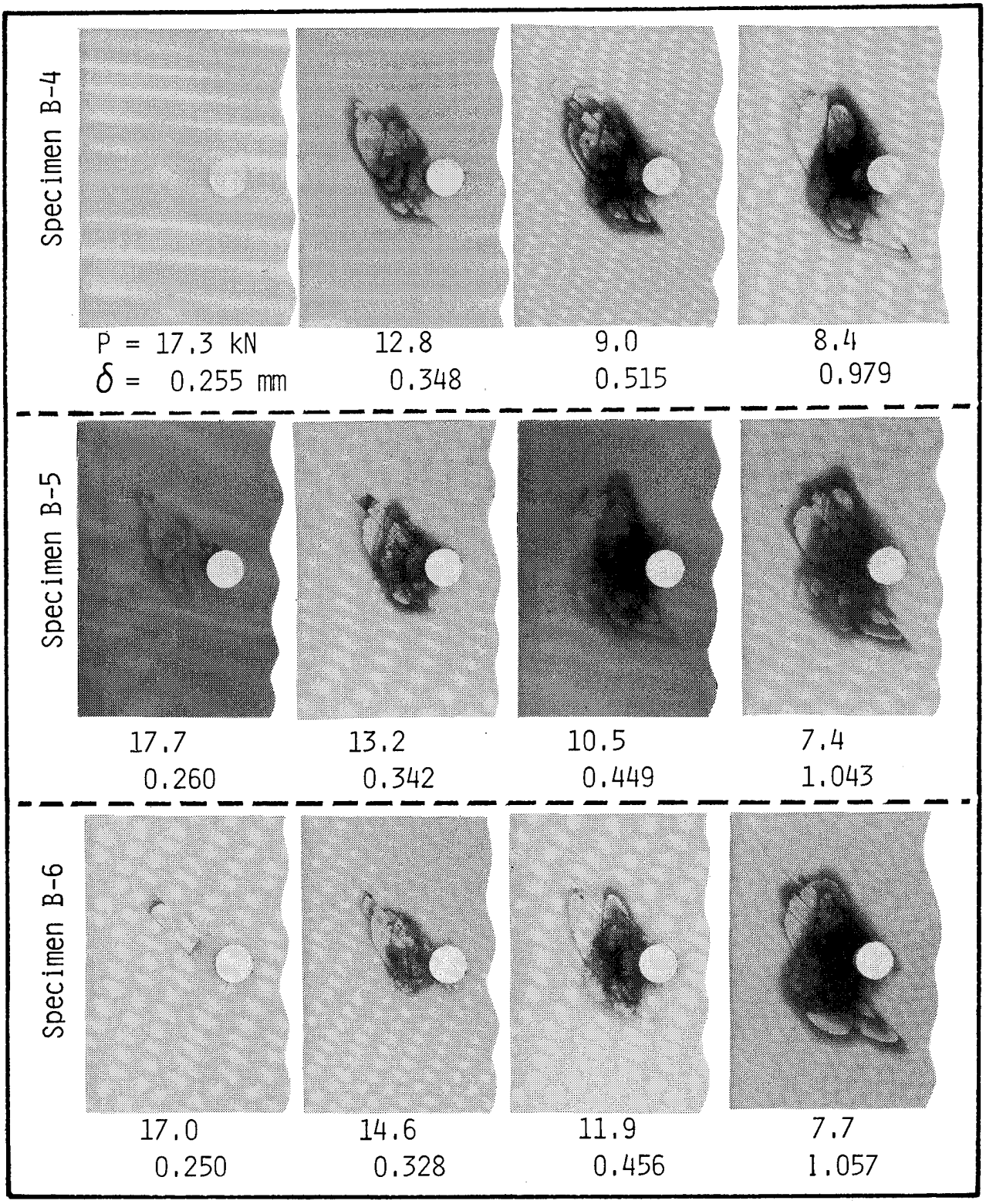

(b) 25-percent bonded.

Figure 21. Continued.

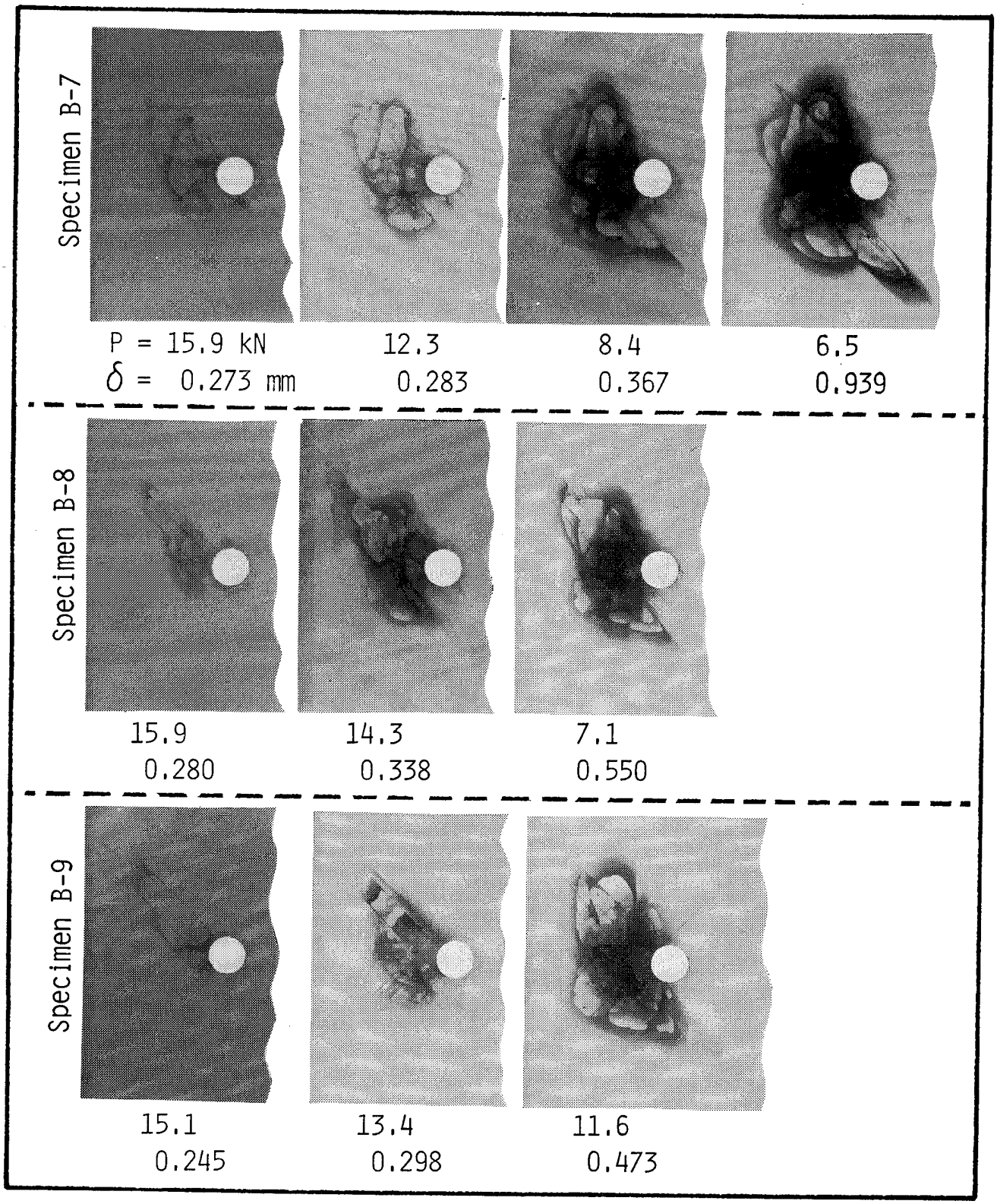

(c) 15-percent bonded.

Figure 21. Concluded.

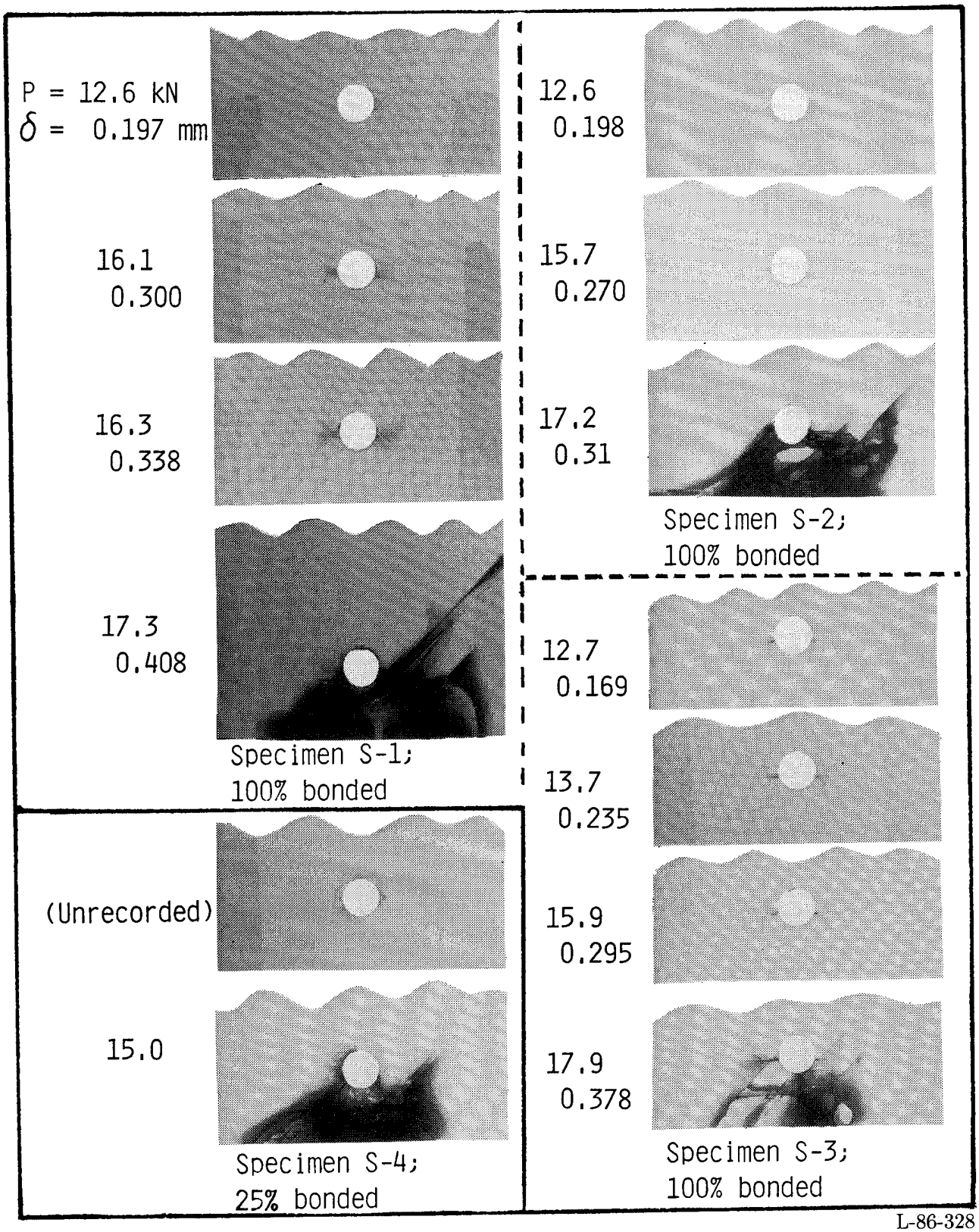

Figure 22. Radiographs of shear-critical specimens. Pin loaded toward bottom; zinc iodide was used as enhancer.

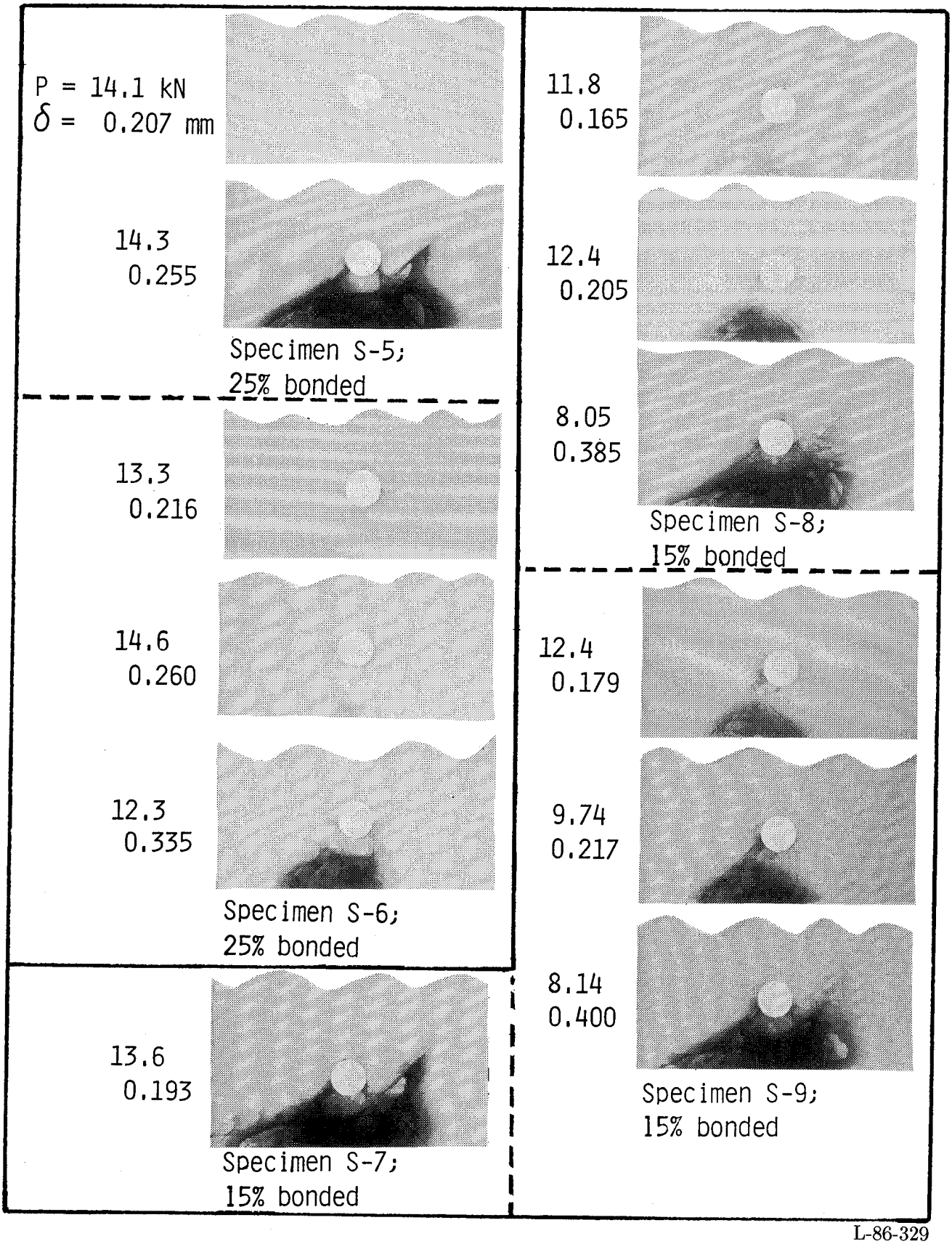

Figure 22. Concluded.

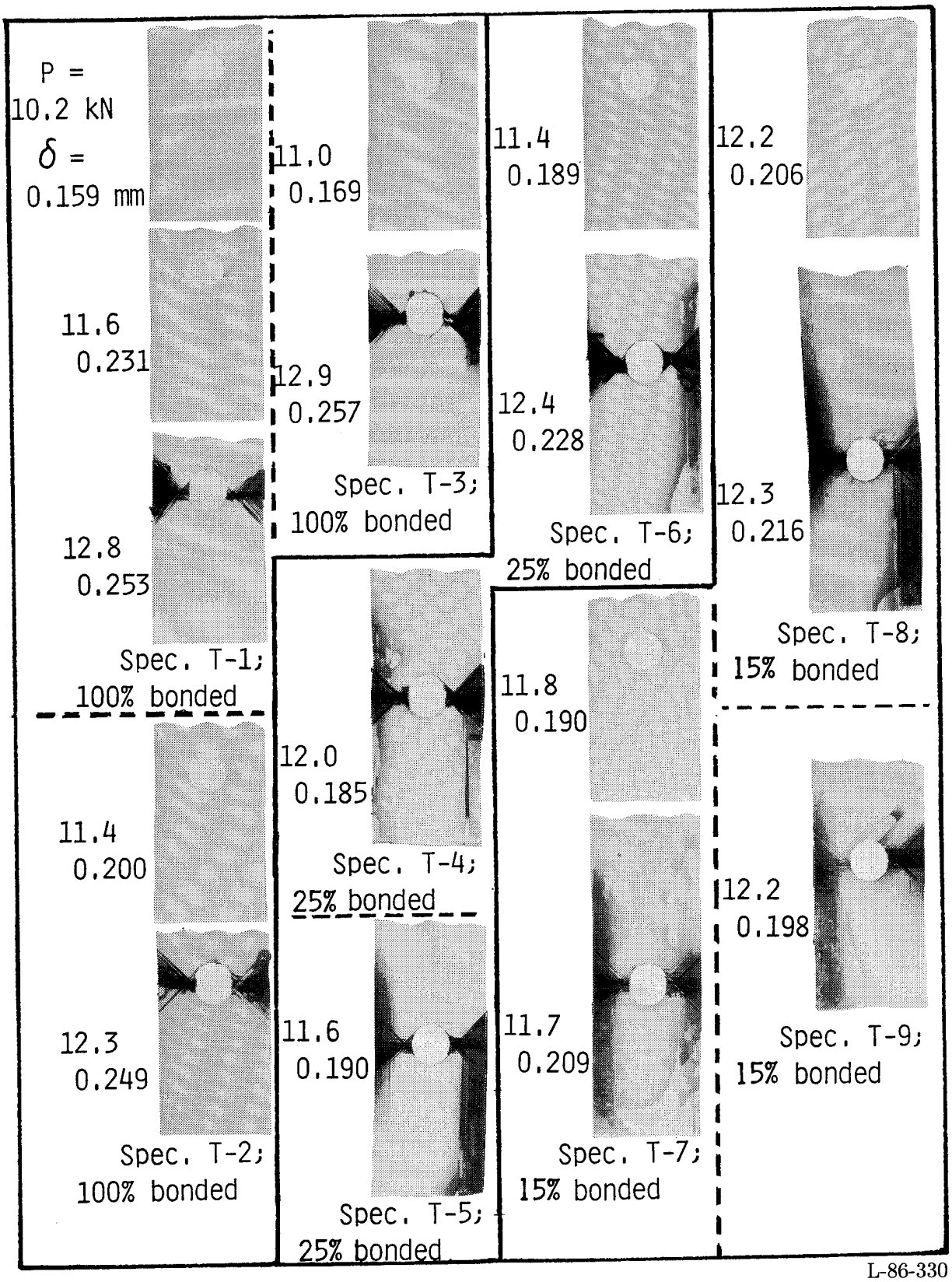

Figure 23. Radiographs of tension-critical specimens. Pin loaded toward bottom; zinc iodide was used as enhancer.

Standard Bibliographic Page

1. Report No.	2. Government Accession No.	3. Recipient's Catalog No.
NASA TM-87678		

4. Title and Subtitle	5. Report Date
Effects of Partial Interlaminar Bonding on Impact Resistance and Loaded-Hole Behavior of Graphite/Epoxy Quasi-Isotropic Laminates	July 1986
	6. Performing Organization Code: 506-43-11-04
7. Author(s): Walter Illg	8. Performing Organization Report No.: L-16088
9. Performing Organization Name and Address: NASA Langley Research Center, Hampton, VA 23665-5225	10. Work Unit No.
	11. Contract or Grant No.
12. Sponsoring Agency Name and Address: National Aeronautics and Space Administration, Washington, DC 20546-0001	13. Type of Report and Period Covered: Technical Memorandum
	14. Sponsoring Agency Code

15. Supplementary Notes

16. Abstract

A partial-bonding interlaminar toughening concept was evaluated for resistance to impact and for behavior of a loaded hole. Perforated Mylar® sheets were interleaved between all 24 plies of a graphite/epoxy quasi-isotropic lay-up. Specimens were impacted by aluminum spheres while under tensile or compressive loads. Impact-failure thresholds and residual strengths were obtained. Loaded-hole specimens were tested in three configurations that were critical in bearing, shear, or tension. Partial bonding reduced the tensile and compressive strengths of undamaged specimens by about one-third. For impact, partial bonding did not change the threshold for impact failure under tensile preload. However, under compressive preload, partial bonding caused serious degradation of impact resistance. Partial bonding reduced the maximum load-carrying capacity of all three types of loaded-hole specimens. Overall, partial bonding degraded both impact resistance and bearing strength of holes.

17. Key Words (Suggested by Authors(s))	18. Distribution Statement
Composition Impact damage Residual strength Graphite/epoxy Interleaf	Unclassified—Unlimited Subject Category 24

19. Security Classif.(of this report)	20. Security Classif.(of this page)	21. No. of Pages	22. Price
Unclassified	Unclassified	47	A03

For sale by the National Technical Information Service, Springfield, Virginia 22161

NASA-Langley, 1986